FOLLOWER FORCE EXPERIMENTS WITH GEOMETRIC NON-LINEAR COUPLING FOR ANALYTICAL VALIDATION

THESIS

Tae H. Kim, Captain, USAF

AFIT/GA/ENY/11-M10

DEPARTMENT OF THE AIR FORCE
AIR UNIVERSITY

AIR FORCE INSTITUTE OF TECHNOLOGY

Wright-Patterson Air Force Base, Ohio

AFIT/GA/ENY/11-M10

FOLLOWER FORCE EXPERIMENTS WITH GEOMETRIC NON-LINEAR COUPLING FOR ANALYTICAL VALIDATION

THESIS

Presented to the Faculty

Department of Aeronautics and Astronautics

Graduate School of Engineering and Management

Air Force Institute of Technology

Air University

Air Education and Training Command

In Partial Fulfillment of the Requirements for the

Degree of Master of Science in Astronautical Engineering

Tae H. Kim, BS

Captain, USAF

March 2011

AFIT/GA/ENY/11-M10

FOLLOWER FORCE EXPERIMENTS WITH GEOMETRIC NON-LINEAR COUPLING FOR ANALYTICAL VALIDATION

Tae H. Kim, BS

Captain, USAF

Approved:

// signed //	18 Mar 2011
Dr. Eric D. Swenson (Chairman)	Date
// signed //	18 Mar 2011
Dr. Donald Kunz (Member)	Date
// signed //	18 Mar 2011
Lt. Col. Kevin J. LaRochelle (Member)	Date

Abstract

This study was a follow-up of a previous study where static deflection data of a joined-wing test article was collected from a series of experiments using a laser scanner and a laser tracker while the test articles were subjected to follower-forces. One of the goals of this study was to collect accurate experimental data which could be used to validate analytical methods, such as geometrically exact beam theory, which are used to predict the nonlinear response of joined-wings. The load application system used on the previous study was not able to provide a follower-force on the test articles, and therefore the loads were not representative of what the joined-wing would experience under more realistic loading conditions. The test articles used for the experiments are the qualification model and the joined-wing model. The qualification model is simply a thin aluminum beam, which is 72 in long, 8 in wide, and 0.5 in thick, and the joined-wing model is made up of two aluminum beams, which are similar in dimension to the qualification model and are joined at the tip. The qualification model was used mainly for validating the experimental procedures in preparation for the actual experiment on the joined-wing model. The deflection data of the test articles were collected using a laser tracker, and some of the measurement locations were chosen for easy comparison with the results from the previous study. The experimental data is compared to the results obtained using finite element analysis to determine how close the finite element analysis predictions are to the actual data.

Acknowledgements

I would like to thank my wife for always being there.

Tae H. Kim

Table of Contents

List of Figures

Page

List of Tables

Page

FOLLOWER-FORCE EXPERIMENTS WITH GEOMETRIC NONLINEAR COUPLING FOR ANALYTICAL VALIDATION

1. Problem Statement

High Altitude Long Endurance (HALE) Intelligence, Surveillance, and Reconnaissance (ISR) aircrafts are a valuable military asset, which can be used for persistent presence over an area of interest. HALE aircrafts operating environment necessitates wings with high aspect ratios that provides high lift with low drag, but are still light weight and stiff. The Global Hawk, a current generation HALE Unmanned Aerial Vehicle (UAV), is capable of providing 24 hours of on-station surveillance of a target 1200 nm away from base, and it is desired to increase the loiter time to several days for future generation HALE UAVs. One of the design concepts being considered for use on future HALE UAVs is the joined-wing concept, which was patented by Wolkovich[1] in 1986 as an alternative to the conventional wing design. The joined-wing concept offers some possible benefits over conventional designs such as the ability to house a 360 degree radar, higher stiffness wings, and potential for increased fuel storage. However, due the inherent geometric nonlinearity of the static response for the joined-wing design, the analysis and optimization of the joined-wing design can prove to be challenging and somewhat risky.

Nonlinear response of the joined-wing is encountered when the wing experiences large deformations. Even with the added stiffness that the joined-wing design provides, the high aspect ratio wings will experience large deformation that cannot be accurately predicted with linear analysis. The design of the joined-wing itself makes it inevitable that the deformation of the wing will involve bending and twisting of the fore and aft wings. The nature of the actual aerodynamic loads causes the direction of the force to change with the deformation of the wings, referred to as a follower-force. Both the bend-twist coupling and follower-force necessitate nonlinear analysis.

Over the years, there have many analytical studies on the joined-wing design. These studies concluded that nonlinear analyses are required for the joined-wing design efforts, which typically means that significant computational resources are required to accurately model the behavior of the joined-wing. As a result there are efforts to find alternative methods for analysis, nonlinear and linear, that will hopefully reduce the required time and resource for accurate analysis of the design. Regardless of whether the analysis is completed by using traditional approaches like finite element analysis (FEA), or

new approaches such as geometrically exact beam theory (GEBT) or equivalent static loads (ESL), analysis results need to be validated through experiments. The lack of the experimental data is the result of the difficulty of conducting an experiment that can match the boundary conditions of the analytical setup.

The objectives of this research are threefold. The first objective is to design, analyze, and build a follower-force load application structure capable of safely applying loads that can be changed as the test article deforms. The second objective is to collect static response data from a qualification and joined-wing test articles subject to follower-forces. The third is to compare static response of the test articles under non-follower and follower-force loads.

The research follows-up on the work of Boston[2] on the same set of test articles, but with follower-forces applied to them. The two types of test articles used for the experiment are the qualification model and the joined-wing model. The qualification model is basically a simple cantilever beam, which is used to establish the standard experiment procedures that are to be used for the experiments on the joined-wing model. The joined-wing model will be used to obtain experimental data that are to be used for validation of analytical tools. In addition to experiments, FEA is used to obtain analytical results for comparison with the experiment data, and the differences in the effects of follower and non-follower forces on the test articles are evaluated.

2. Background

This chapter gives a short background on the joined-wing concept and reviews some of the studies that have been conducted on the concept. The lessons learned from the experimental studies are incorporated into this thesis research, and lack of experimental data available for comparison with analytical studies is a motivation for the thesis research.

The joined-wing design, as described by Wolkovich in his Journal of Aircraft article in 1986, combines tandem wings arranged to form diamond shape in both plan and front views.[1] The advantages claimed for a properly designed joined-wing included light weight, high stiffness, low induced drag, good transonic area distribution, high trimmed C_L max, reduced wetted area and parasitic drag, direct lift control capability, direct side force control capability, and good stability and control. An optimization study by Gallman and Kroo of mid-range transport mission aircraft showed that a joined-wing design would cost more to operate due to possible buckling problems and inability of creating maximum lift during takeoff[3]. However, their study does point out that its focus was on the mid-range transport missions, and that the joined wing design may prove to perform better than the conventional design in a different type of mission.

The Air Force Research Lab (AFRL) Air Vehicles Directorate has funded research of a joined-wing HALE sensorcraft, with the objective of exploring optimal configurations to maximize endurance and radar coverage, and to minimize weight and cost. HALE sensorcraft's mission will require it to fly long duration ISR missions at high altitudes. As a result, such an aircraft will have high aspect ratio for aerodynamic efficiency and will require as much area as possible for sensors. The advantage of the joined-wing design over the conventional one for this purpose is that the aft wings of the joined-wing design will provide additional stiffness in the wings and additional surface area for the sensors. Research from AFRL has shown that structural optimization of the joined-wing design is possible through analytical means and that nonlinear structural analysis of joined-wing design is necessary.[4] However, since limited experiments have been carried out to validate the analysis, experimental data of nonlinear behavior of a joined-wing is very much desired.

2.1 Previous Experimental Studies

There have been several studies where experimental data has been collected for comparison with analytical results. Most of the experiments have had problems which made it difficult to compare the experimental data to the analytical data. However, those problems have produced lessons learned, which allows others to avoid similar problems in future studies.

In the experimental study by Bond [5], one of the objectives was to demonstrate the nonlinear behavior inherent in the joined-wing configuration, then to validate the FEM analysis method of such structures by comparing the experimental and analytical results. Using a system of cables, turnbuckles, and weights, Bond created a follower-force setup in an attempt to simulate realistic loads experienced by actual aircraft wings. Tension scales were used to measure the load applied at the tip, displacement probes were used to measure displacements at three points, and strain gauges were used to obtain strain data at 14 points. The load was applied to the test article by tightening the turnbuckles, and at each load increment the deflection and strain data were taken. The initial results showed similar nonlinear behavior in both the experiment and the FEM, but large discrepancy in deflection and strain; the test article was shown to be 40% more flexible than the FEM. Further investigation showed that the assumed fixed boundary condition for the experiment was most likely suspect. By changing the fixed boundary condition at the roots of the wings in the FEM, Bond was able to decrease the discrepancy between the experimental and analytical results. Bond's work demonstrated a method of applying follower-force to a joined-wing test article and demonstrated the importance of correctly modeling boundary conditions.

Figure 2.1: Bond Test Article (CAD Model)

Green, Keller, and Boston [6] conducted an experiment to analyze an aluminum joined-wing model obtained from AFRL. The object of the study was to predict the nonlinear geometric bending and

twisting of the test article as shown in the analytical research accomplished by AFRL. Since the aluminum test article was welded on to a sturdy base, the fixed boundary condition was assumed for the FEM. The test loads were applied at two different points, with two load cases at each point. Green *et al.* had difficulty matching the experimental data to the analytical results, but discovered that changing the value of the Young's modulus improved the agreement between the two results, which led them to suspect that the test article might have yielded. Although analysis of the loads applied showed that stresses on the structure should be below the yield limits, Green *et al.* concluded that unwittingly applied impulse loads must have cause the test article to yield. Upon closer investigation of the test article, it was discovered that the welded joint between the fore and aft wing was cracked, which likely contributed to the discrepancy in the data. Their study shows that yielding of the test article must be taken into account during testing and that it would be important to check for yield after each test load.

(a) (b)

Figure 2.2: Green *et al.* (a) Test Article and (b) Test Article Load Points

Dreibelbis and Barth [7] tested three different joined-wing configurations made from aluminum bars 1 in wide and 1/8 in thick. The first configuration, referred to as the planar wing, had a 20 in fore wing and an aft wing of half the length attached midway along the fore wing. Unlike the joined-wing configuration studied in this thesis research, the wings were located in the same plane. The second configuration, called the bi-planar wing, had the same fore wing, but the aft wing was offset 3 in along the direction normal to the plane of the fore wing and the wings were attached together by a vertical piece. In the third configuration, called the non-planar wing, the fore and the aft wings were attached directly like the first configuration, but the root of the aft wing was offset 3 in along the direction normal to the plane of the fore wing. In all cases, the roots of the wings were clamped to simulate a fixed boundary condition and the load was applied by hanging various weights from the tip of the fore wing. The static

displacements were measured at two points: the joint where the wings come together and at the tip of the front wing. Comparisons were made between the experimental data and FEA results. The experimental data showed that the bi-planar and non-planar wings were stiffer than the planar wing, and although the data on the single fore wing is not presented in their paper, Dreibelbis and Barth concluded that the addition of the aft wing significantly increases the stiffness of the joined-wing compared to the just the fore wing by itself. An interesting outcome of the experiment is their conclusion "that a nonlinear relationship between the deflection and the applied load does not exist" in the joined-wings tested.

(a) (b) (c)

Figure 2.3: Dreibelbis and Barth Test Articles (a) Planar, (b) Bi-Planar, and (c) Non-Planar

After his work with Green, Boston[2] conducted an experiment to obtain accurate experimental data which could be used to validate results obtained using analytical methods. The experiment setup incorporated the lessons learned from works by Bond, Dreibelbis and Barth, and Green *et al.* Boston designed the experiment to ensure that the boundary conditions could be reproduced easily by ensuring that the assumption of fixed boundary conditions at the wing roots are valid. He also analyzed FEMs of various dimensions to determine the joined-wing dimensions that would display bend-twist coupling prior to material yield. Finally, Boston made sure to check for material yield in the test articles by taking zero load measurement at the beginning and the end of each experiment.

The experiment was conducted in two phases using qualification and joined-wing test articles. The qualification test article is a simple aluminum beam 72 in long, 8 in. wide, and 0.5 in. thick. The joined-wing test article is made up of the fore wing with chord width of 8 in. and the aft wing with chord width of 6 in. The vertical distance from the root to the tip of the joined-wing, where the fore and aft wings are connected, is 57 in. Boston used the qualification test to verify that his procedure would give the desired data prior to conducting tests on the joined-wing test article.

(a) (b)

Figure 2.4: Boston Test Articles (a) Qualification and (b) Joined-Wing

He measured static deflections of his test articles using a laser tracker for point measurements and laser scanner for surface displacement measurements. While all data points measurements collected with the lasers were used to make direct comparisons with a node on the FEM, the surface scans also proved useful in providing a visual comparison with the FEA results. The experimental data showed that the movement of the wing roots was negligible, proving his fixed boundary condition assumption correct. Boston was also able to closely match the experimental data with the results of nonlinear analyses from the FEA of the joined-wing test article.

Boston's work shows a way of ensuring that an assumption of a fixed boundary condition for the roots of the joined-wings is valid, and provides a test article that will display geometrically nonlinear behavior before yield. One improvement that can be made to his work is to change the loading system so that a follower-force can be applied to the joined-wing to reflect a more realistic loading condition, which is one of the aims of this thesis research.

2.2 Previous Analytical Work

As with most design analysis, much of the work on the joined-wing concepts has been done with analytical tools rather than through actual experiments. In most cases, the design studies involve both linear and nonlinear analyses, and compare the results obtained from the two approaches. Linear analysis is preferred in regards to computational resource requirements since results are obtained relatively quickly. However, most studies seem to indicate that nonlinear analysis is a necessity if accurate results are desired. As a result, there are efforts to find way quicker ways of obtain similar results as those given by

nonlinear analysis, whether it is by utilizing new methods of nonlinear analysis or by using linear analysis in a way that will yield the same result given by nonlinear analysis.

The objective of Marisarla's[8] research was to produce a ANSYS version of the "box-wing" model, an in-house Sensorcraft joined-wing model developed by AFRL in NASTRAN. The "box-wing" model is an equivalent representation of the actual joined-wing model, which is idealized as a box structure consisting of shells, rods, beams, shear panels, and concentrated masses. As a result, this model requires less computational resources over the full 3-D model of the joined-wing. By converting the NASTRAN model into an equivalent ANSYS model, the research sought to validate the procedure used in creating the "box-wing" model while producing an accurate model of the joined-wing that could be analyzed using ANSYS. There was discrepancy in the results computed from the two analysis tools, which stemmed from the different approaches that the two software programs took when it came to attaching different types of elements together. The discrepancy between the results computed by the two software programs for the same analyses showed the importance of understanding the workings of the FEA tools in order to properly utilize them. It also showed how valuable it would have been to have actual experimental data available for comparison, so that it would be possible to determine which of the two results, if any, was correct.

Narayanan's[9] research focused on the joined-wing model made of shell elements that had the identical shape as the aerodynamic model of the Sensorcraft wing. Of the two models created, the first model used the same surface discretizations as the computational fluid dynamics (CFD) model so that loads of the CFD analysis could be directly applied to the FEA analysis. Due to the discretization method used on the first model, there were problems with the elements at the leading and trailing edges of the wing, which made it impossible to conduct a nonlinear analysis using FEA. The second model was created to rectify this problem. Nonlinear and linear analyses on the second model with various loads showed that difference between the analysis results increased as the applied loads increased. Nonlinear analyses also showed deformation in the wings skin at the roots, which were absent in the linear analysis results. Narayanan concluded that inclusion of nonlinear effects is required for accurate study of the joined-wing's aeroelastic behavior.

Kaloyanova[10] modeled the joined-wing as a semi-monocoque structure, where the aerodynamic pressure loads are shared by the wing skin and underlying supports, rather than a monocoque structure, where all of the loads are sustained by the skin. First, analysis was conducted on a model with uniform material distribution and then model optimization was performed to reduce the stresses and the deformation of the wing. The first analysis showed that the max stress found on the wing was exceeding

the ultimate stress of the wing material. After the optimization, the max stress on the wing was below the yield limit and the max deflection was less than the first case. Kaloyanova conducted linear and nonlinear analysis for both models, and the results indicated that the linear analysis yields more conservative results. This was also true of the linear and nonlinear buckling analysis conducted on the optimized model, where the results showed that the linear analysis predicts a higher load for the onset of buckling. Kaloyanova concluded that although the difference between linear and nonlinear analysis results were not great for loads considered in the study, the use of nonlinear analysis is necessary to accurately predict the deformation and buckling that would result from more realistic loads experienced by actual wings.

Ramussen[11] conducted a study of various joined-wing configurations by varying six design variables: front & aft wing sweep angle, horizontal & vertical offset distance of the wing roots, fractional joint location of the wing, and thickness to chord ratio. The goal of his study was to obtain a general relationship between each of the design variables through automated nonlinear analyses so that an optimal weight configuration of a joined-wing design could be determined from those relationships. Although he was not able to determine exact optimal configurations using the relationships he found, he was able to isolate regions where the optimal configurations were located. Of the 3 optimal configurations found, 2 were "in-plane" configurations where there was no vertical offset between the roots of the fore and aft wing. It was found that the joined-wing configurations tended toward large vertical offset with low thickness-to-chord ratio, where global buckling was a concern, or toward small vertical offset with high thickness-to-chord ratio, where panel buckling was more of an issue.

Patil[12] developed a nonlinear aeroelastic analysis methodology and used it to analyze two of the joined-wing models, planar and non-planer, tested by Dreibelbis and Barth[7]. The methodology makes use of a geometrically exact structural model for dynamics of beam-like structures and combines it with various aerodynamic models in order to investigate nonlinear aeroelastic behavior of the joined-wing design. The linear and nonlinear analysis produced results which were close to one another and to the experimental results, but were not able to capture the yield behavior observed during the experiment. It was found that the joined-wing models were significantly stiffer than a single wing, and the presence of the aft wing gave the joined wing a better resistance to torsion. However, further analysis showed that buckling is a concern as the thickness of the aft-wing decreases due to the compressive load on it. He concluded that nonlinear behavior in the structures were negligible, as indicated in his results, and his work again shows that joined-wing design that is too stiff will not display nonlinearities before yield.

Blair, Canfield, and Roberts[4] conducted an optimization study on a joined-wing design with the goal of obtaining certain level of aerodynamic performance while remaining below acceptable structural

stress levels in static aeroelastic equilibrium. Linear and nonlinear optimized models were developed and analyzed for various loads that the joined-wing might experience during flight and on the ground. Buckling analysis showed that the joined-wing configuration displays large geometric nonlinearity below critical buckling eigenvalue, which suggested that nonlinear analysis was required to correctly model the geometry. The load case corresponding to landing loads showed that the front wing could also be susceptible to buckling. Blair *et al.* successfully optimized joined-wing designs for various load cases and demonstrated the possibility of converging a structurally optimized and aerodynamically trimmed conceptual joined-wing design. They expressed confidence in the integrity of their optimization process, but expressed the need for experimental validation of the results.

Adams[13] evaluated the Boeing Joined-Wing SensorCraft design to determine its dynamic modes, ensure buckling safety, and determine the effects of nonlinearities. The nonlinearities considered were those resulting from the geometry of the design and follower-force loads. His study determined that the SensorCraft design was not weight optimized, and as result the wing was overly stiff. As a result of this stiffness, nonlinearity effects were not significant, expected deformations were small, and global buckling was not a critical condition. He concluded that although global buckling was not an issue for the Boeing design, it will be a concern for weight optimized designs.

Green's[14] study involved merging of two analysis methods to obtain optimization results similar to those obtained through conventional nonlinear analysis. He used a variant of the GEBT, a formulation of beam theory that can accurately capture the combined bending and twisting (bend-twist) of beams, and ESL, where static loads are used to simulate nonlinear responses. The nonlinear response of the simple model studied was obtained from GEBT, the result was converted to ESL for linearized optimization, and the optimized design from ESL was analyzed by GEBT to check for convergence. Although there were occasions Green's results and those obtained from conventional nonlinear methods of analysis were different, most of the results showed that use of GEBT and ESL for optimization has potential for greatly reducing the computational resources required for nonlinear analysis.

The above studies sought to accurately analyze and find ways to optimize the joined-wing design using conventional and nonconventional methods of analysis. Most of the analytical studies mentioned above suggest that nonlinear analysis is required for accurate results, but their studies do not have comparisons of their nonlinear analysis results against experimental data. Whether it is for cases where results from different FEA tools are compared or where results from nonconventional and conventional methods are compared, the actual experimental data would be valuable in validation or correction of the

analysis tools. However, since such experimental data are not as readily available, this research seeks to collect them for use in validation of the analytical methods used for joined-wing design.

3. Methodology

3.1 Experimental Setup

The experiment was conducted in two stages using two different test articles. The first stage was conducted using the qualification model to establish the experiment procedures that are later used on the second stage of the experiment. The experiments on the joined-wing model are conducted in order to collect experimental data, which could be used to validate analytical methods used for analyzing the joined-wing design.

In order to apply a follower-force on the test articles, a test stand capable of changing the load application direction was built. The load was applied to the test articles by the use of pulleys, cables, and a winch, with a load cell to determine the magnitude of the load applied. The displacement measurements of the test article were collected at various points using a laser tracker, and the correct orientation for the follower-force load was determined through vector calculations using the laser point tracker data.

3.2 Qualification Test Article

The qualification test article is a solid 6061 aluminum beam with dimensions 8 in x 0.5 in x 72 in (width x thickness x length). In order to apply a load to the test article, mounting structures, made out of 4130 steel, are attached to the top and bottom of the test article, as shown in Figure 3.1. The top mounting structure provides an attachment point for the cable, which is used to apply the load, and the bottom mounting structure is used to attach the entire test article to a base plate, which is bolted to the ground and functions as a fixed boundary condition. These top and bottom mounting structures provide the added benefit of serving as the transition for the applied loads and rigid boundary conditions to reduce stress concentrations. The attachment of all parts of the test article is done with bolts, which allows easy assembly and disassembly as necessary. The base plate is secured to the concrete floor using six 0.5 in bolts, which are each rated to resist 8,000 lbs of pullout force. The six bolts should be sufficient to ensure fixed boundary conditions, however, in order verify that the assumption is valid the movement of the base is monitored during the experiments.

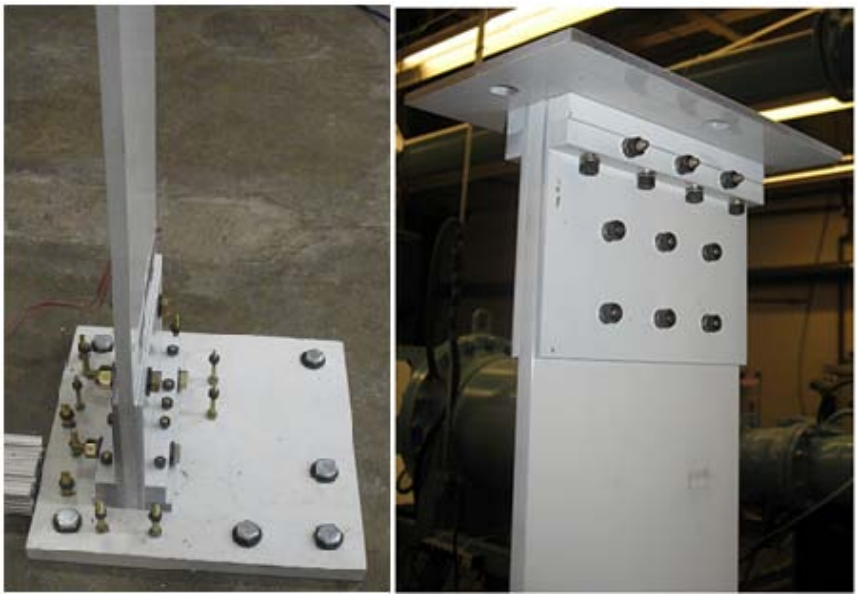

(a) (b)

Figure 3.1: Mounting Structures (a) Bottom and (b) Top

The load is applied using a cable that is connected to a winch rated to 1500 lbs. The load cell is connected in between the test article and the cable in order to accurately measure the load being applied, as shown in Figure 3.2. The test article was loaded from 25 lbs to 200 lbs in 25 lb increments using follower-force loads. Non-incremental follower-force loads of 125 lbs, 150 lbs, 175 lbs, and 200 lbs were also applied for comparison with the data obtained from incremental loads. The purpose of the comparison was to determine whether incrementally loading the test article to a particular load has any different effect than directly loading the test article to the same load.

Figure 3.2: Qualification Model under a Follower-Force Load

3.3 Joined-wing Test Article

The joined-wing test article was also built using the same solid 6061 aluminum beams, and its shape is shown in Figure 2.4(b). The dimensions of the fore wing are 8 in x 0.5 in x 67 in (chord x thickness x span), with the dimensions of the aft wing differing only in the chord dimension, which is 6 in. As with the qualification model, top and bottom mounting structures, made out of 4130 steel, are attached to the wings to provide a fixed boundary condition and a load application point, but the top plate in this case also serves as a joint for the fore and aft wings (Figure 3.3). The overall height of the joined-wing test article is 57 in. The assembly of the test article is achieved through the use of bolts as in the case with the qualification model. The root of each wing is bolted to a base plate, which secured to the ground with six 0.5 in bolts each. The movement of the base plates is monitored to ensure the validity of the assumption of fixed boundary conditions.

(a) (b) (c)

Figure 3.3: Mounting Structures (a) Top/Joint, (b) Left Bottom, and (c) Right Bottom

The dimensions of the fore and aft wing were determined by Boston[2] through trial and error FEA optimization to satisfy conditions which were found to be problematic in previous experimental studies - designing a structure that clearly exhibits a bend-twist coupling response without yielding at any point on the structure.

The procedure for load application is similar to that used on the qualification model. The joined-wing test article was loaded at 25 lbs, at 100 lbs, and then up to 1100 lbs in 100 lb increments with follower-force loads. As with the qualification model experiments, non-incremental follower-force loads directly to 1100 lbs were applied so that comparison with the incremental load data could be made. An example of the joined-wing test article under load is shown in Figure 3.4.

Figure 3.4: Joined-Wing Test Article under Load

3.4 Follower-Force Load Application System

In order to apply a follower-force on the test articles, it is necessary to have the ability to change the direction of the applied force as the test articles deform. Since the decision was made to use cables and pulleys to apply the load, one end of the cable is attached to the load application point on the test article and the other end ("free end") needs to have two degrees of freedom to allow the direction of the load to vary. The additional requirement on the "free end" of the cable is that its location needs to remain fixed once the desired load direction is obtained. In order to satisfy both conditions required of the "free end" of the cable the test stand shown in Figure 3.5 was built.

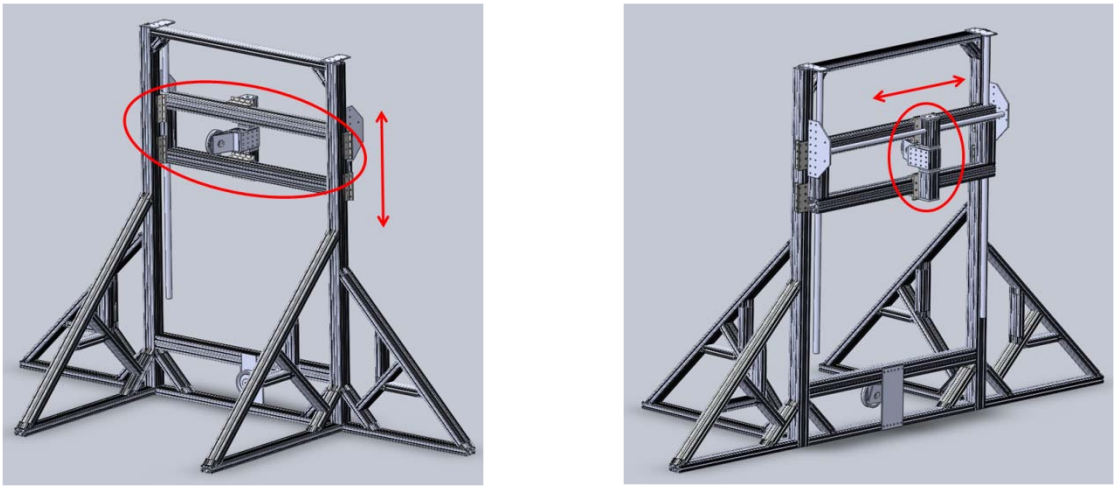

(a) (b)

Figure 3.5: Test Stand (a) Front View and (b) Rear View

The test stand is basically a rectangular frame that has supports on the sides and front. It is built using 80/20 aluminum beams since a variety of accessories is available which makes the creation of arbitrary structures relatively easy. The main rectangular frame supports a smaller rectangular frame that translates vertically on sliders to provide the first degree of freedom. The smaller rectangular frame supports a vertical component with a pulley that translates horizontally on sliders to provide the second degree of freedom. The middle section of the horizontally translating vertical component is capable of rotating to provide yet another degree of freedom, which was at first thought to be necessary (Figure 3.6). However, when FEA results for the joined-wing model using follower-forces were used to predict the location of the pulley, it was shown that horizontal movement required for the pulley was about an inch for a 1200 lbs load. This is shown in Figure 3.7 where the horizontal and vertical distances for the pulley are measured with respect to the bottom left corner of the main rectangular frame. The figure includes positions for loads up to 1500 lbs and the point corresponding to 1100 lbs is labeled. Although the deflection of the actual test article under various loads was different from the FEA predictions, the horizontal adjustments of the pulley remained within couple of inches of the initial position. Due to the relatively small amount of displacement in the horizontal direction, the degree of freedom provided by the rotation of the vertical section attached to the pulley was constrained since it proved to be unnecessary for the test articles concerned in this study.

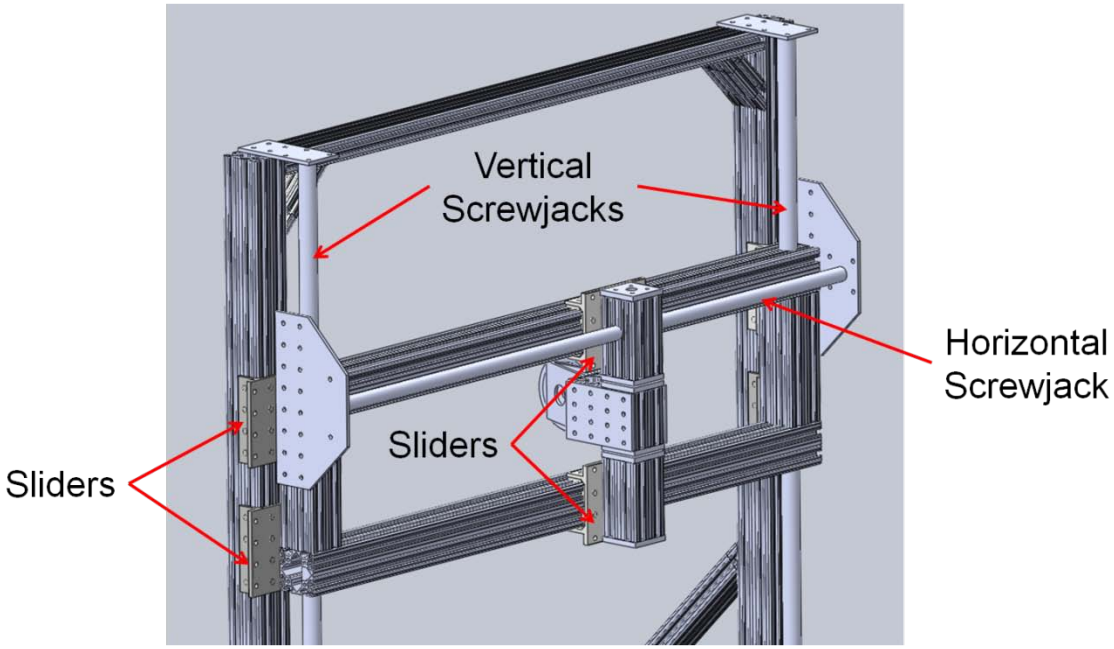

Figure 3.6: Translating Sections of the Test Stand

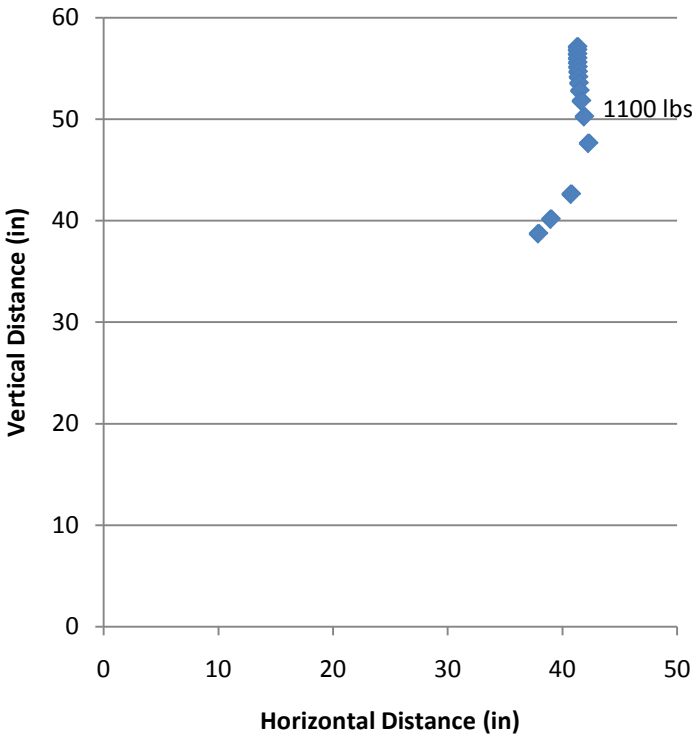

Figure 3.7: Predicted Location of the Pulley

The mechanisms for vertical and horizontal translations of the pulley were provided by screwjacks with traveling nuts. The screwjacks were ideal for this purpose since in addition to providing the precisely controlled translations, they also were capable of maintaining the desired position. Two 2-ton capacity screwjacks (vertical screwjacks) were connected together using couplings and a shaft so that they would turn in sync. The traveling nut on each of the screwjacks was bolted onto the smaller rectangular frame so that it would translate vertically as the screwjacks were turned. One 1-ton capacity screwjack (horizontal screwjack) was used to provide the horizontal translation of the vertical component supported by the smaller rectangular frame. As was done with the smaller rectangular frame, the vertical component was bolted on to the traveling nut of the horizontal screwjack so that turning the screwjack would result in its translation. An inch of vertical translation equates to 24 turns on the vertical screwjack's input shaft, and an inch of horizontal translation equates to 25 turns on the horizontal screwjack's input shaft. The horizontal and vertical screwjack setups are shown in Figure 3.8.

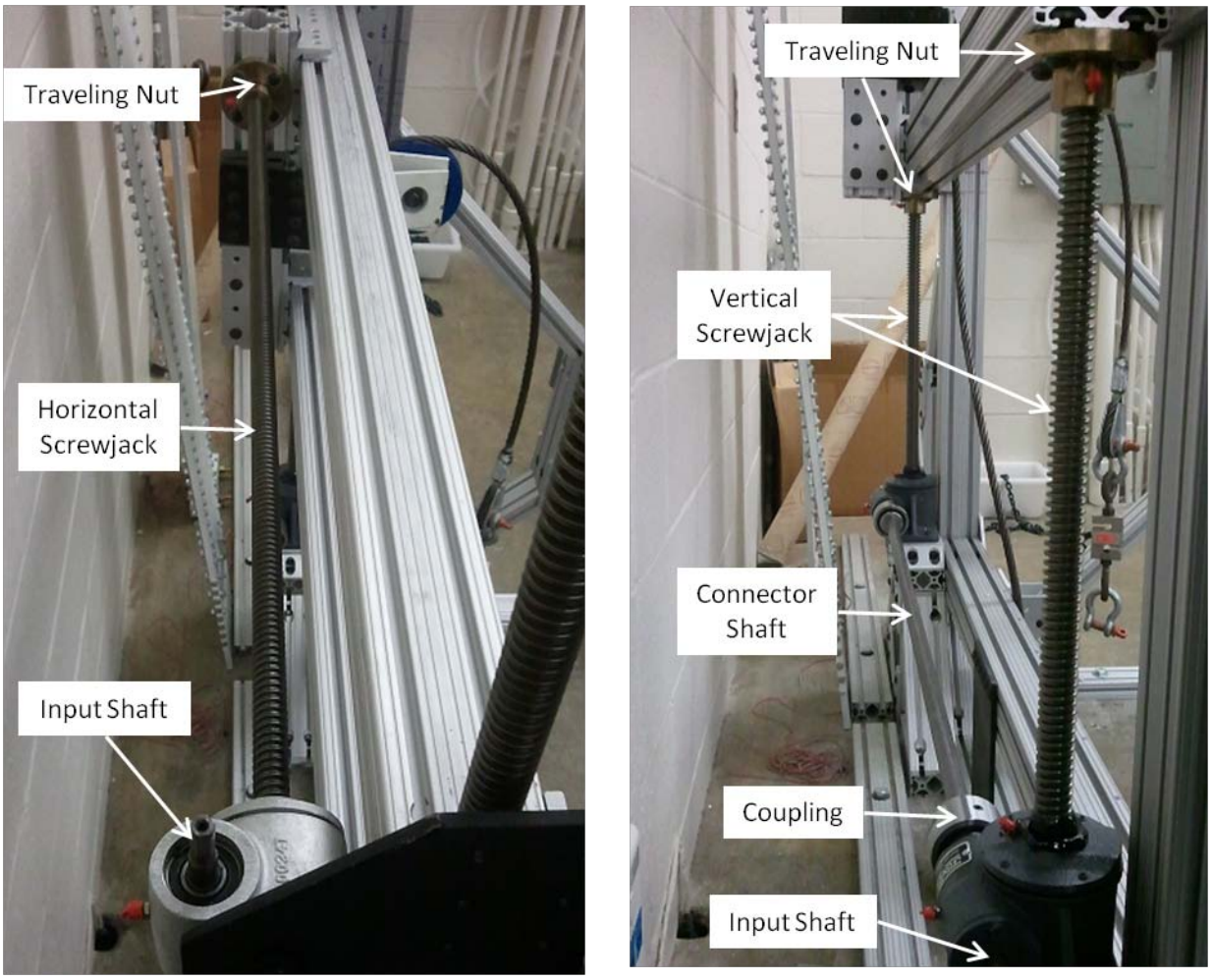

(a) (b)

Figure 3.8: Screwjack Setup for (a) Horizontal Translation and (b) Vertical Translation

The load is applied to the test article through a 1/2 in cable, which is attached to a winch capable of providing 1500 lbs of force, and measured using a Sensortronics S-beam load cell attached to IQ plus 355 Digital Weight Indicator. An example of load application on the qualification test article is shown in Figure 3.9, and the load cell and the weight indicator are shown in Figure 3.10. There was a tendency for the load to creep at the higher loads (400 and above), but load adjustments were made to ensure that the value was within 1% of the desired load. The load cell only measures the magnitude of the force being applied, so the direction of the load is determined via laser tracker measurements of the test article. A spreadsheet was used to calculate how close the current load direction is to the desired follower-force direction and to determine how much the pulley must be moved horizontally and vertically for the actual and desired load directions to align. The method used to determine whether follower-force load is being applied to the test articles is discussed in the following section.

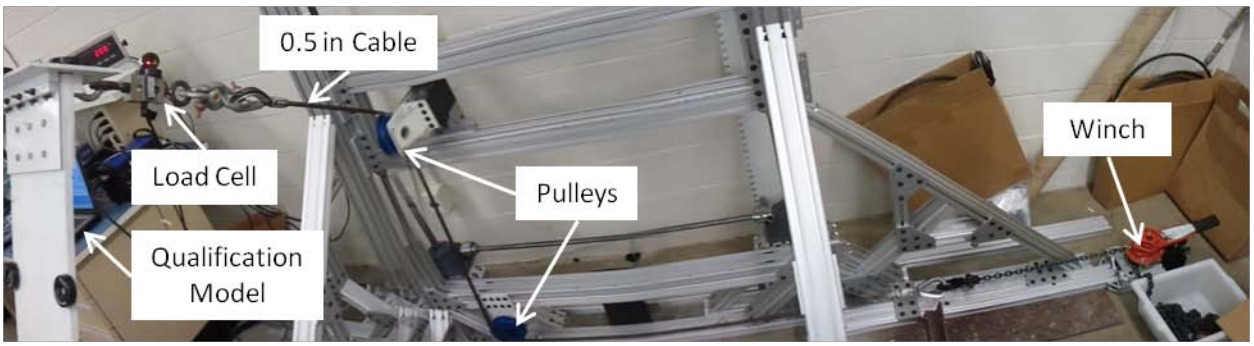

Figure 3.9: Load Application using Cable, Pulleys, and a Winch

(a) (b)

Figure 3.10: Load Measuring Instruments (a) Load Cell and (b) Weight Indicator

FEA was conducted on a simple model of the load application system both before and after it was built. The analysis before the construction of the load application system was necessary to determine whether the 80/20 material would be capable of withstanding the loads that were going to be applied to the test articles. The analysis after the construction of the load application system was necessary since some changes were made to the design. The changes to the design were motivated by the actual materials that were available for the construction of the load application system.

The static load FEA results for the load application system for maximum load case on the qualification and joined-wing test articles are shown in Figure 3.11 and Figure 3.12. The maximum stresses predicted are 594 and 3,421 psi for the qualification and joined-wing models, respectively, which are well below 35,000 psi, the yield strength of the material. The model of the load application system is created using simple beam elements with cross sectional information of the 80/20 aluminum beams. The major difference between the load application system and the FEA model of the system is the simplification that the translating sections are modeled as one connected piece that is a part of the main rectangular frame of the load application system. However, since the screwjacks are capable of

preventing the translating sections of the load application system from moving, the simplification should be appropriate.

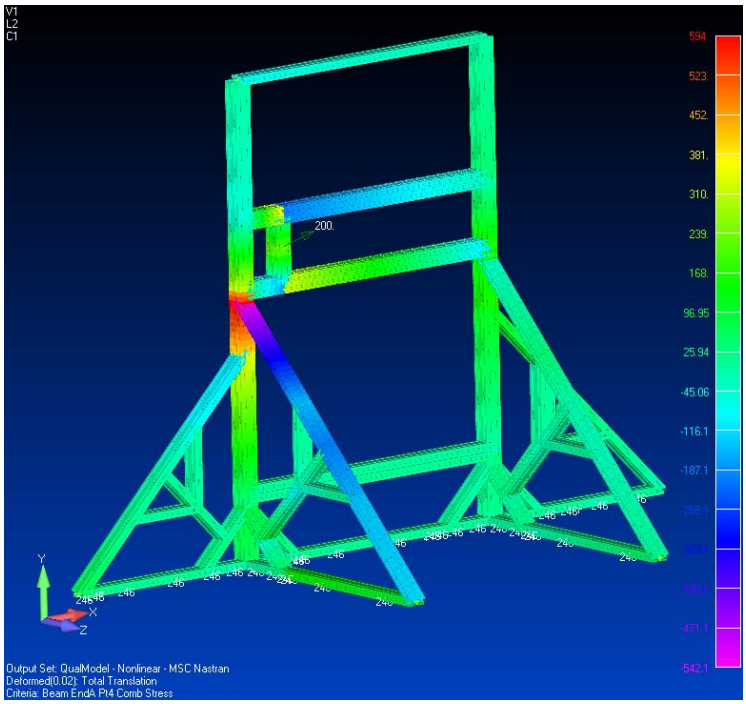

Figure 3.11: Stress Predicted When Applying Maximum Load to the Qualification Test Article

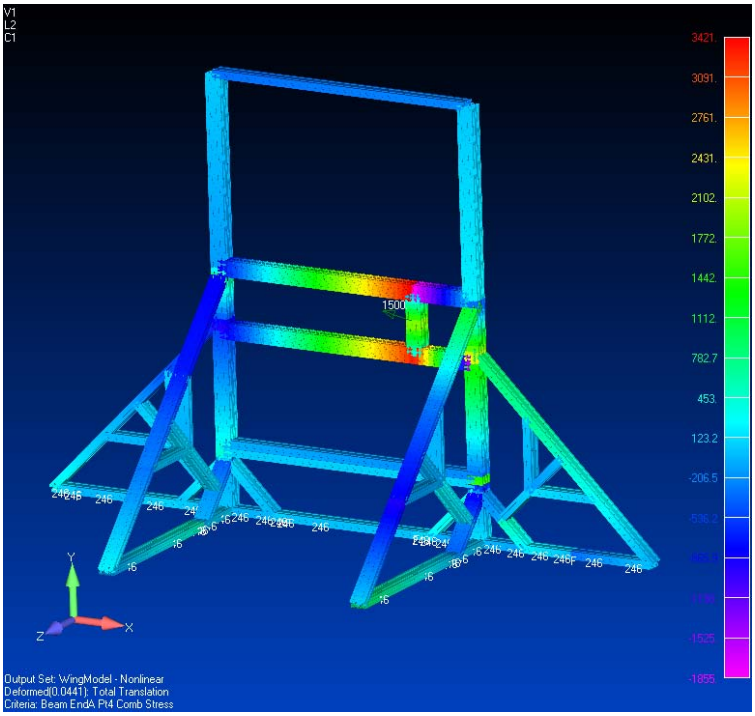

Figure 3.12: Stress Predicted When Applying Maximum Load to the Joined-Wing Test Article

Since a maximum load of 1200 lbs was planned to be applied to the joined-wing, it was necessary to make sure that the load application system would remain fastened to the ground. The load application system was secured in 6 different places with the same 0.5 in bolts used for the base plates of the test articles in order to ensure that it would not come loose during load application.

3.5 Strain Gages

In Boston's[2] study, strain gages were placed in locations where the largest stresses were predicted by FEA analysis. Since the same test articles are being used for the current study, the strain gages have not been removed and they were used to take strain measurements during the experiments. The strain measurements were used to ensure that the test article did not yield under the loads applied during the experiment.

The qualification model contains three strain gages, but only two were used for the current study, and the joined-wing model has four strain gages. The gage locations are shown in Figure 3.13.

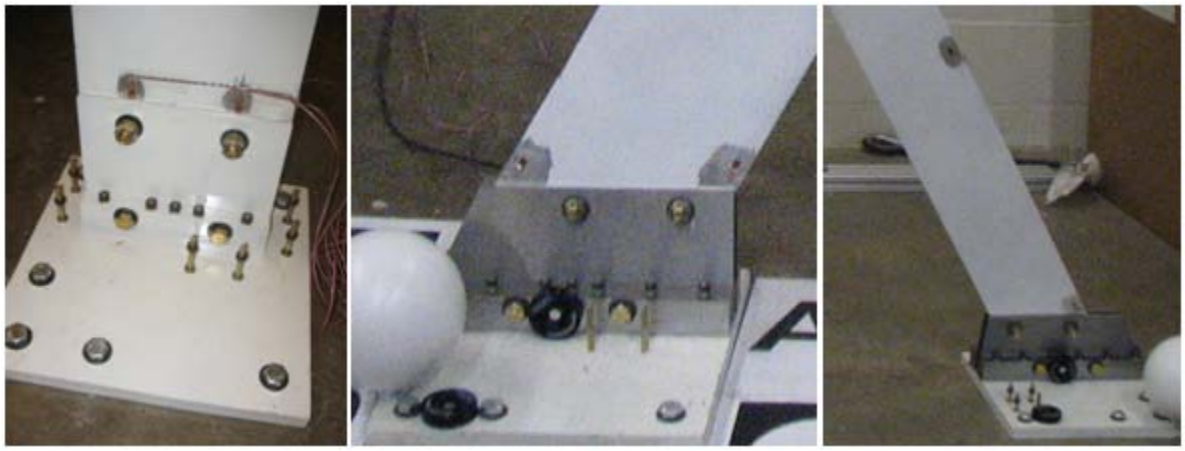

(a) (b) (c)

Figure 3.13: Strain Gage Locations (a) Qualification, (b) Fore Wing, and (c) Aft Wing

3.6 Collecting Measurements.

The test article displacement measurements are taken with the FARO Laser Tracker Xi, which measures position in three dimensional space by sending out a laser to the spherically mounted retroreflector (SMR), shown in Figure 3.14, and receiving the reflected beam. The calculation of the position data is obtained from the radial distance, horizontal angle, and vertical angle measurements, and the tracker is able to provide typical accuracy of about 0.02 mm (0.0008 in) at 10 m range to the target.

The mounts for the SMR are hot glued onto the test article at desired measurement locations as shown in Figure 3.15.

(a) (b)

Figure 3.14: (a) FARO Laser Tracker Xi (b) SMR

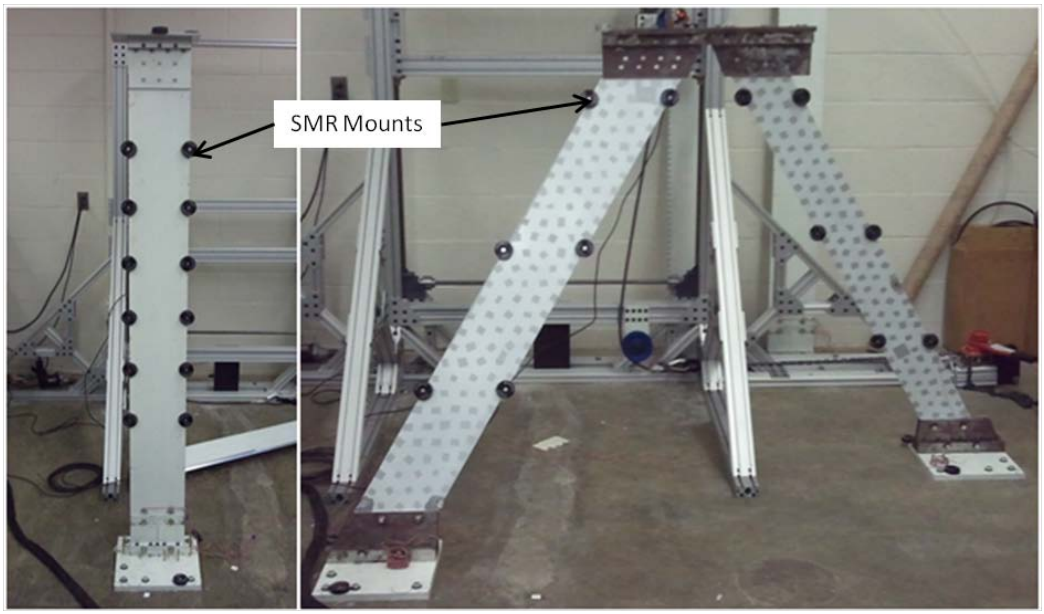

(a) (b)

Figure 3.15: SMR Mounts on Test Articles (a) Qualification and (b) Joined-Wing

In order to account for possible permanent deformations, the test articles were always measured before any load was applied to them. Along with measurements collected at the unloaded state, strain measurements and additional measurements of two reference points at the base of the main rectangular frame of the loading application system were taken so that the data sets could be compared even if the laser tracker was moved. During the experiment, the displacement and strain measurements were

collected after the desired load was applied to the test article. After the max load were applied, the test articles were unloaded and measured again so that data would be available to check for any permanent deformations and ensure any slippage is removed.

Since the input shaft for the vertical screwjacks and the winch are located on opposite sides of the load application system, it was not possible for one person to change the direction of the load and maintain a constant load on the test article at the same time. Therefore, when it was necessary to increment the load on the test article, the load was first increased to the desired value by turning the winch and then the direction of the load was changed as necessary by changing the pulley position with the screwjacks. However, since changes in the pulley position affect the load that the cable applies to the test article, it was necessary adjust the load again to the correct value using the winch. At this point, laser tracker measurements were collected and the spreadsheet was used to check for alignment. If further adjustments were necessary, the pulley position was adjusted as indicated by the spreadsheet, the required load was applied to the test article using the winch, and alignment was checked by taking measurements with the laser tracker.

In order to determine whether the sequential process used to load the test articles has any effect on the deformation, the test articles were also loaded directly to the maximum load from the unloaded position so that comparisons could be made between measurements under direct and incremental loads.

3.7 Determination of Load Direction

The follower-force for this study is defined to be a force that remains in the plane defined by the top plate and perpendicular to the left edge of the top plate, as shown in Figure 3.16. The orientation of this follower-force with respect to the top plate does not change as the test article deforms (Figure 3.17). This is different from the load that Boston[2] applied to the test articles during his study (Figure 3.18(a)) or the stationary direction loads that are usually applied in cantilever beam analysis (Figure 3.18(b)). Both of the forces shown in Figure 3.18 have the same initial direction as the follower-force applied to the test articles during this study. However, since the location of the pulley in Boston's load application structure was fixed, the direction of the applied force on the test articles changes with deformation. In the case of the stationary direction force the direction is defined to be constant so that the initial orientation is maintained even when test articles deform.

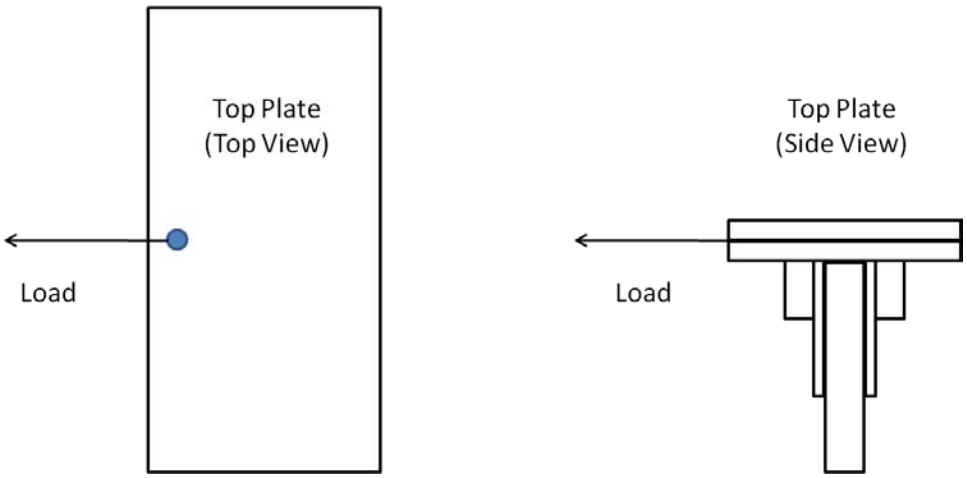

Figure 3.16: Follower Force Definition

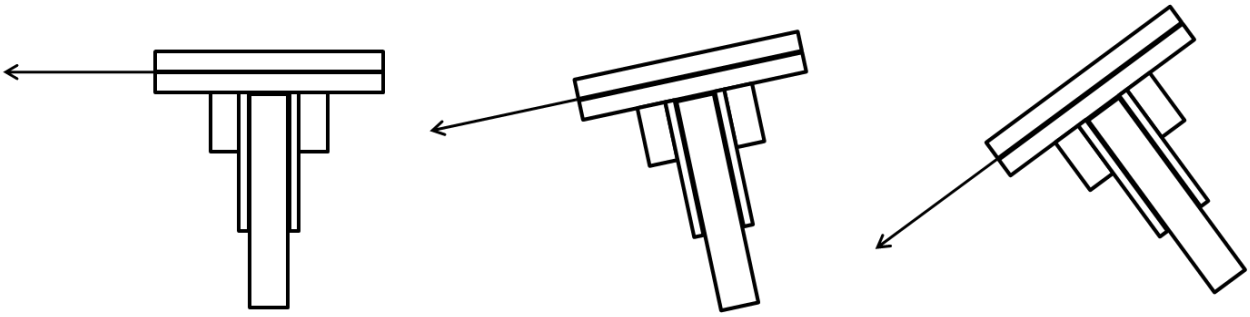

Figure 3.17: Follower-Force Orientation with Deformation

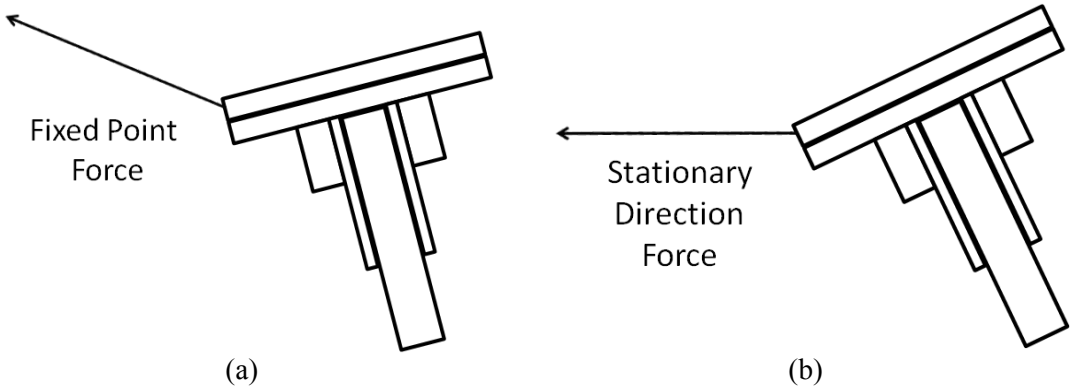

Figure 3.18: Non-Follower Forces - (a) Fixed Point Force and (b) Stationary Direction Force

The determination of the correct follower-force load orientation is made by using vector calculations based on the laser tracker point data. Figure 3.19 shows the basic load geometry for the qualification model. Data points 1 and 2 are located along direction corresponding to the follower-force direction. When follower-force is achieved, the perpendicular distance of point 4 from the top of the top

plate is 0.75 in (Figure 3.20). If the position of point 1P, an imaginary point that is also offset 0.75 in perpendicularly from the top plate above point 1, is known, the unit vector between points 1P and 4 should be parallel to the unit vector calculated from points 1 and 2, as shown in Figure 3.21.

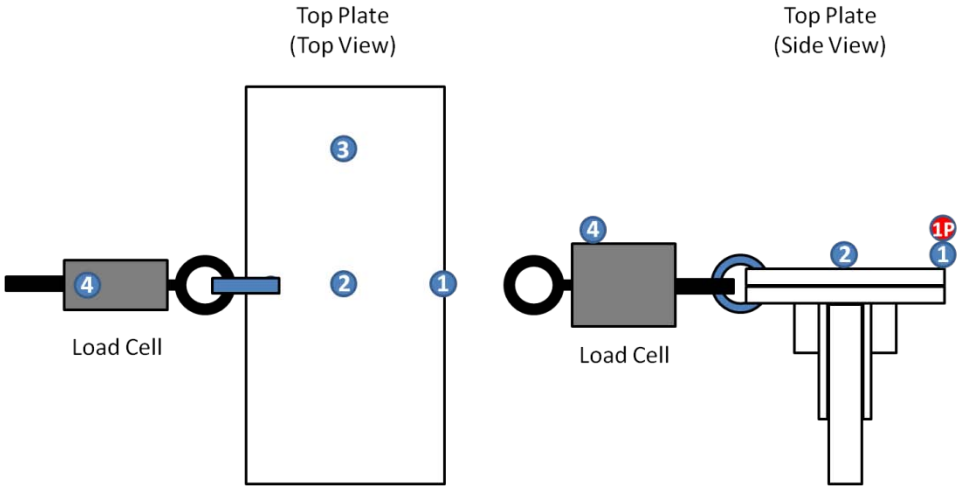

Figure 3.19: Qualification Test Article Load Geometry

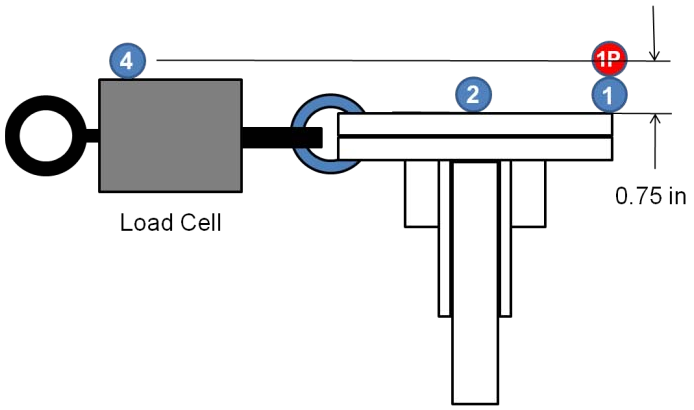

Figure 3.20: Offset Distance of Point 1P

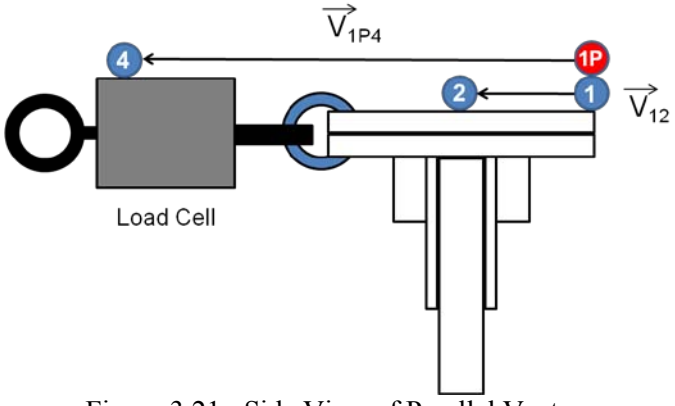

Figure 3.21: Side View of Parallel Vectors

In order to calculate the location of point 1p, unit vectors between points 1 to 2 and points 1 to 3 are first determined (Figure 3.22).

$$\hat{v}_{12} = \frac{\langle p_2 \rangle - \langle p_1 \rangle}{|\langle p_2 \rangle - \langle p_1 \rangle|} \tag{1}$$

$$\hat{v}_{13} = \frac{\langle p_3 \rangle - \langle p_1 \rangle}{|\langle p_3 \rangle - \langle p_1 \rangle|} \tag{2}$$

Then, their cross product is calculated to determine the direction perpendicular to the top plate and a unit vector in this direction is calculated.

$$\hat{n}_{tp} = \frac{\hat{v}_{13} \times \hat{v}_{12}}{|\hat{v}_{13} \times \hat{v}_{12}|} \tag{3}$$

The unit vector is then multiplied by the offset distance, 0.75 in, and added to point 1 to obtain the location of point 1P, as shown in Figure 3.22.

$$\langle p_{1p} \rangle = 0.75\, \hat{n}_{tp} + \langle p_1 \rangle \tag{4}$$

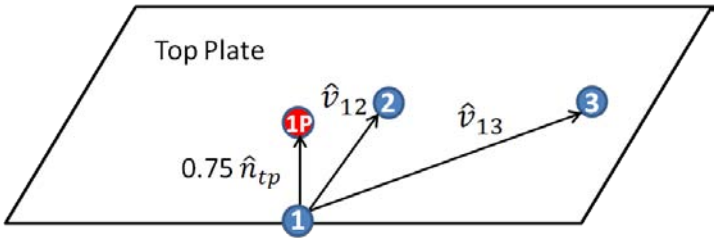

Figure 3.22: Determining the Point 1P

Given point 1P, a unit vector in the direction defined by points 1P and 4 can be determined, and this unit vector can be compared to the follower-force direction represented by points 1 and 2 by evaluating the dot product between the two directions. If the two vectors are nearly parallel, the dot product should be very close to 1 (Figure 3.23). The angle between the actual and the desired load directions will be called the load angle.

$$\hat{v}_{1p4} = \frac{\langle p_4 \rangle - \langle p_{1p} \rangle}{|\langle p_4 \rangle - \langle p_{1p} \rangle|} \tag{5}$$

$$\text{Load angle} = \cos^{-1}\left(\hat{v}_{1p4} \cdot \hat{v}_{12}\right) \tag{6}$$

The criteria used for the follower-force determination was a load direction that is within 1 degree of the follower-load direction. Since cosine of 1 degree is 0.9998, essentially the entire applied load is in the follower-force direction.

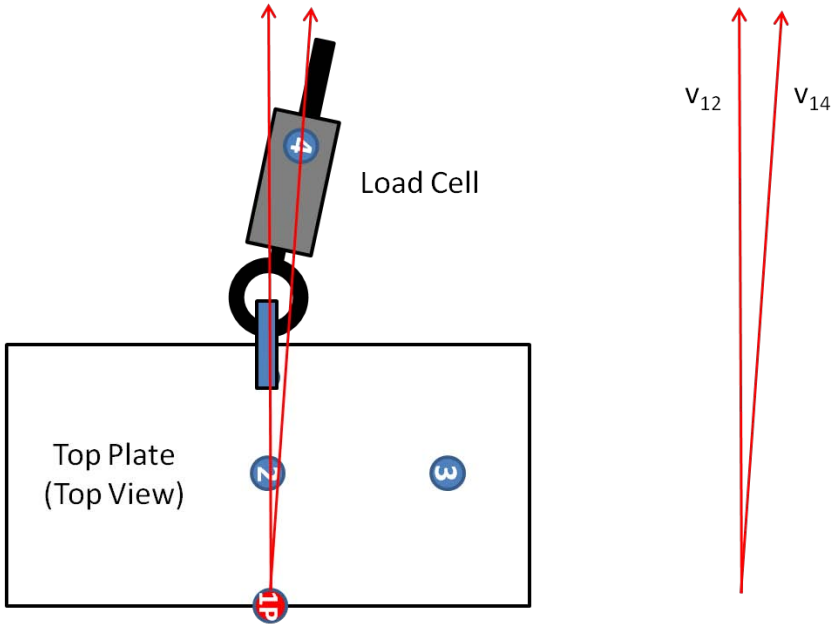

Figure 3.23: Comparing Two Vectors for Alignment

The determination of the correct load orientation for the joined-wing test article is similar, but has couple of differences because the measurement locations are different (Figure 3.24). Points 1 through 3 are still used to determine the unit normal vector to the top plate, but the follower-force direction is defined by the vector perpendicular to the vector from point 1 to point 2. The vector representing the actual load direction is determined from point 4P (a calculated point above point 4 in the normal direction from the top plate) and point 5.

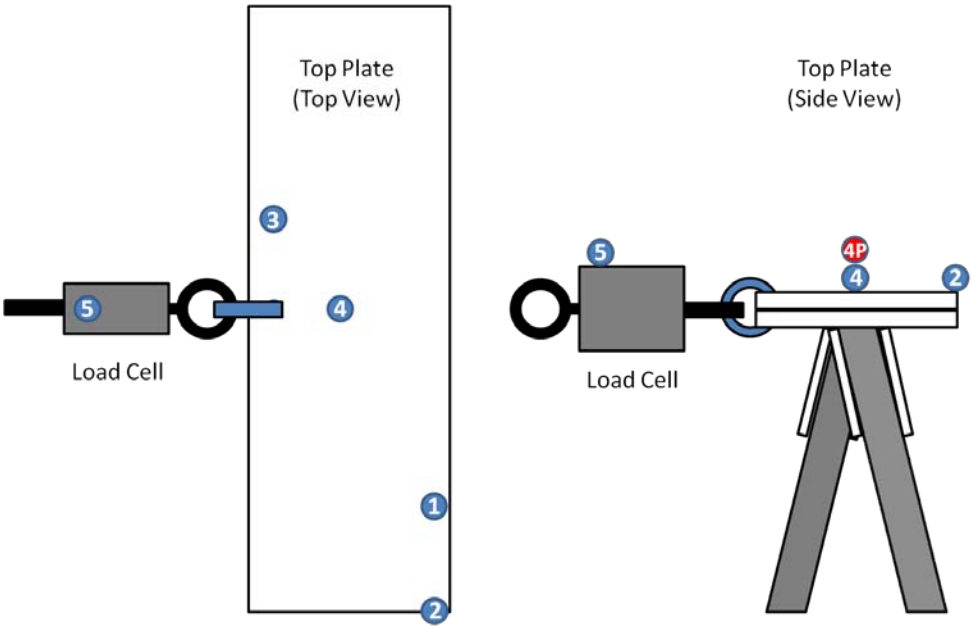

Figure 3.24: Joined-Wing Test Article Load Geometry

The process outlined above makes it possible to determine whether follower-force is achieved to within some tolerance, but does not help in determining what adjustments are needed to get the actual load direction closer to the follower-force direction. If the vector for the cable, along with its pivot location on the test article, was known, simple geometry, as shown in Figure 3.25 and Figure 3.26, could be used to determine the necessary change in horizontal and vertical location of the pulley that would allow the actual load direction to align with the follower-force direction.

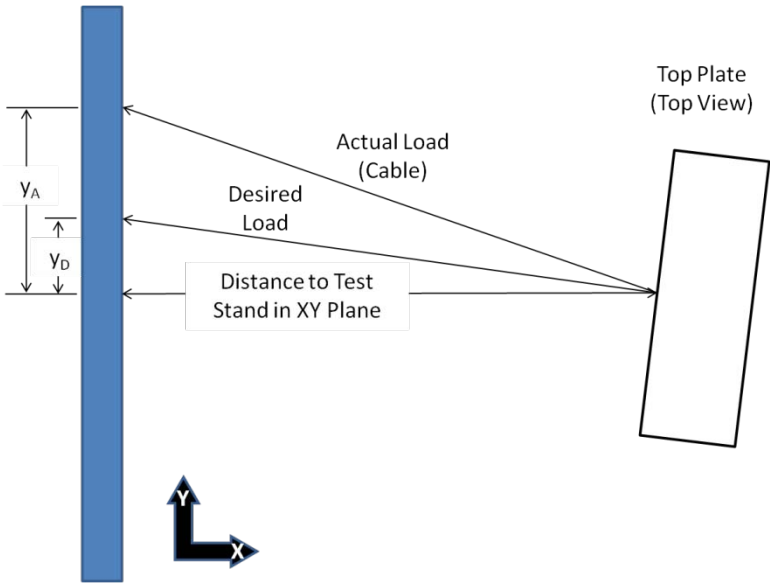

Figure 3.25: Load Direction Comparison (XY Plane)

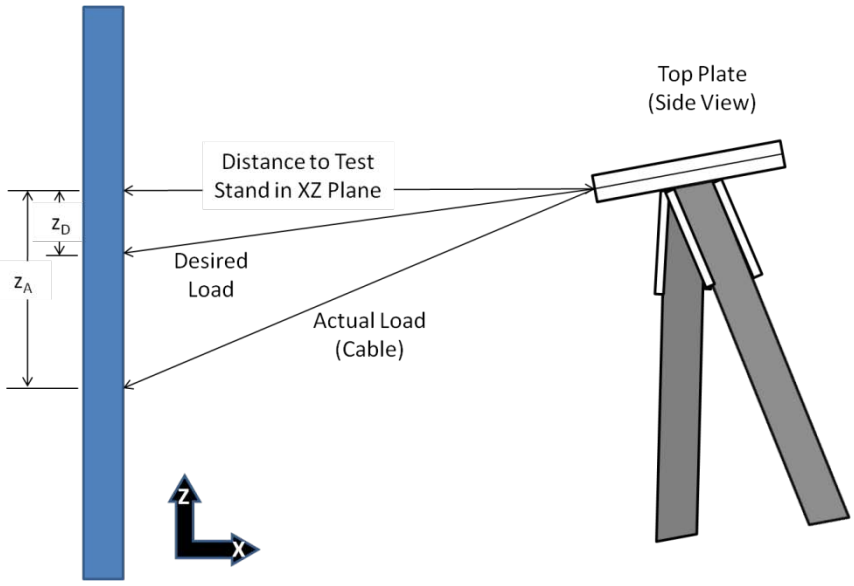

Figure 3.26: Load Direction Comparison (XZ Plane)

The X- and Y-components of the unit vector for the cable along with the distance of the pivot point from the test stand in the X-direction could be used to determine the distance y_A shown in Figure 3.25. The distance y_D is found in the same way using the components of the unit vector in the follower-force direction, and the difference between the two distances will yield the required displacement for the pulley in the Y-direction. Similar process is used in the XZ plane to calculate the necessary vertical displacement. In order to use the process described above, the coordinates of the cable pivot point and the vector for the cable are needed.

The pivot point for the cable is not an actual hard point, but is located between the top plate of the test article and the link connecting the load cell to the test article as shown in Figure 3.27. In the joined-wing test article, its coordinates can be obtained by shifting point 4 toward the top plate along the normal vector by 1.375 in (distance that the SMR is offset from the top plate surface) and then shifting it 3.875 in toward the pivot point in the follower-force direction (perpendicular to the vector defined by points 1 and 2).

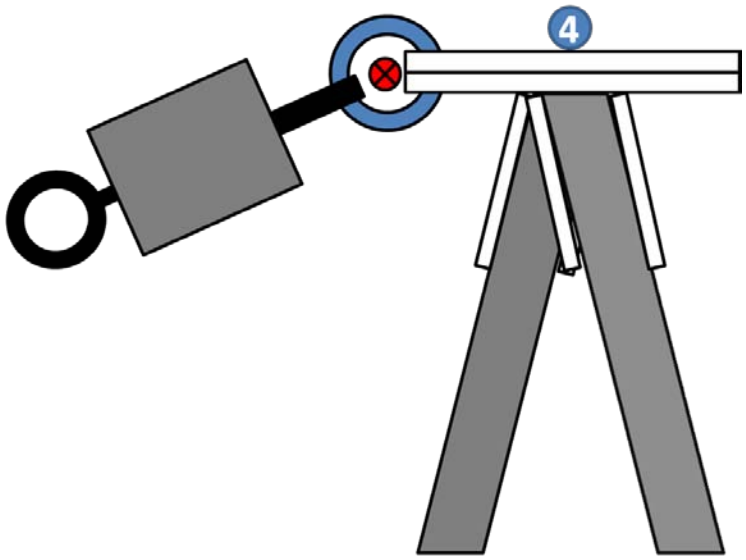

Figure 3.27: Pivot Point of the Cable Attached to the Test Article

Since the only place along the path of the load cable that is capable of providing a place for the SMR mount is on the load cell, it is not possible to take two laser tracker readings along the cable to determine its direction. Therefore, the cable vector is determined by the use of rotation matrices. The cable direction is at first considered to be in the negative X' direction with the Y' axis defined to be in the global XY plane, as shown in Figure 3.28. A rotation about the Y' axis places the X' axis on the XY plane, and another rotation about the Z' direction aligns the X'Y'Z' coordinate system with the XYZ coordinate system. Therefore, a rotation matrix can be constructed to change the cable vector components from the X'Y'Z' coordinates to the XYZ coordinate system if the angles θ and ϕ are known.

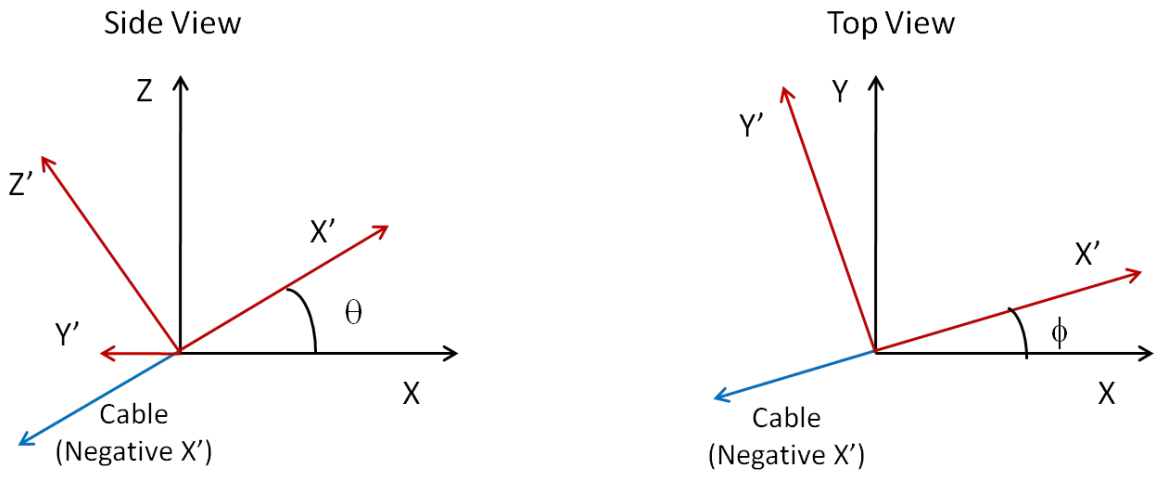

Figure 3.28: Global (XYZ) and Cable Local (X'Y'Z') Coordinate Systems

The angle ϕ is calculated by taking the dot product of negative X-axis with the XY plane projection of the unit vector along the direction defined by the pivot point and the measurement point 5 on the load cell. The angle θ is estimated by first determining β, the angle between the negative X-axis and the XZ plane projection of the vector from the pivot point to point 5 on the load cell as shown in Figure 3.29, and subtracting α from it. The angle α is calculated from the known location of point 5 with respect to the pivot point. Although the exact angle θ is not known, the estimate is enough to approximately determine the necessary vertical adjustment in the pulley position. A lso, since the estimate of θ approaches the true value as the angle ϕ gets smaller, the estimate should improve with each adjustment of the pulley position.

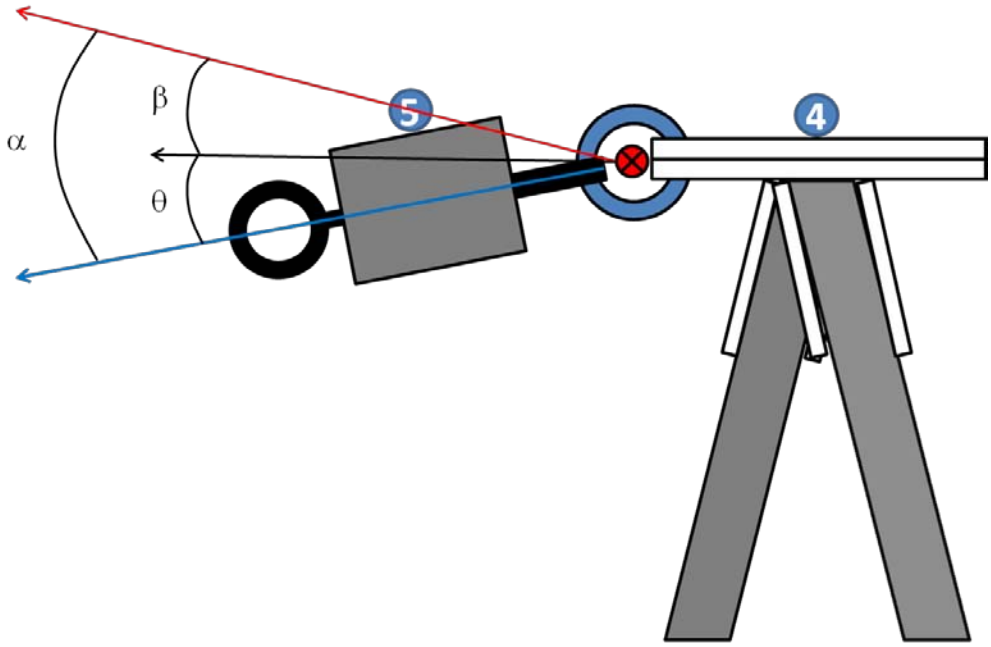

Figure 3.29: Estimating the Angle θ

3.8 Analytical Models.

In order to compare analytical predictions and experimental measurements, follower-forces were applied to the FEMs created by Boston[2] to obtain predicted deformations of the test articles (Figure 3.30 and Figure 3.31). The FEMs of both the qualification and joined-wing test articles consist of QUAD4 elements, with the bolt connections in the top and bottom mounting structures modeled by using 6 degree-of-freedom (6DOF) spring elements (Figure 3.32). The spring elements, rather than rigid links, were used because it was determined that the rigid links made the model too stiff, and because the springs make it p ossible to adjust the stiffness of the model to better fit the experimental data. Assumptions

included in the FEMs are that the materials used for the actual test articles are homogeneous and that bolt connections would act like stiff springs.

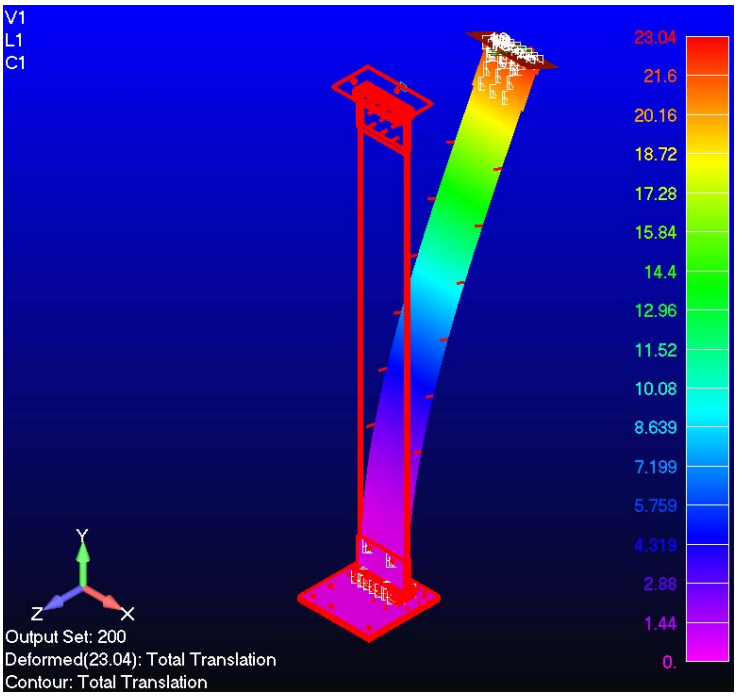

Figure 3.30: Qualification FEM

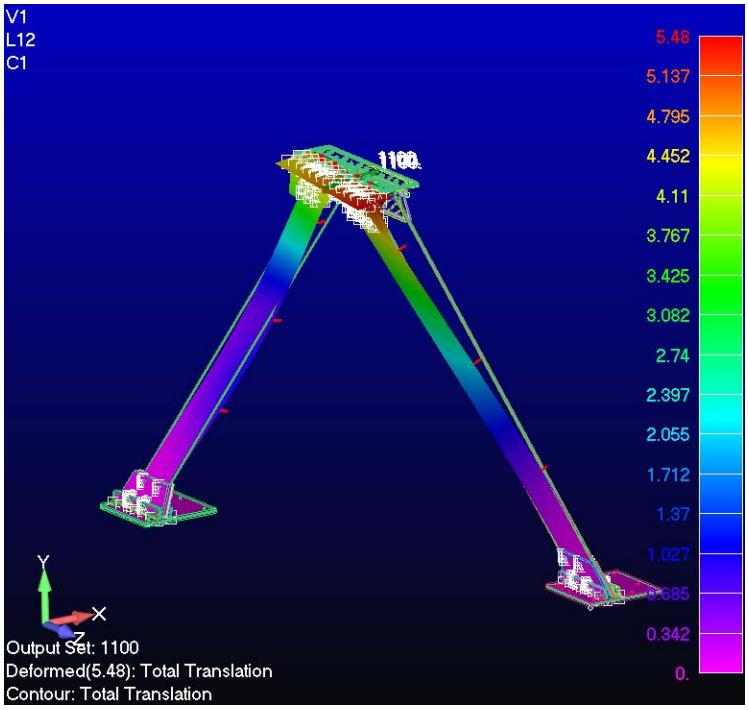

Figure 3.31: Joined-Wing FEM

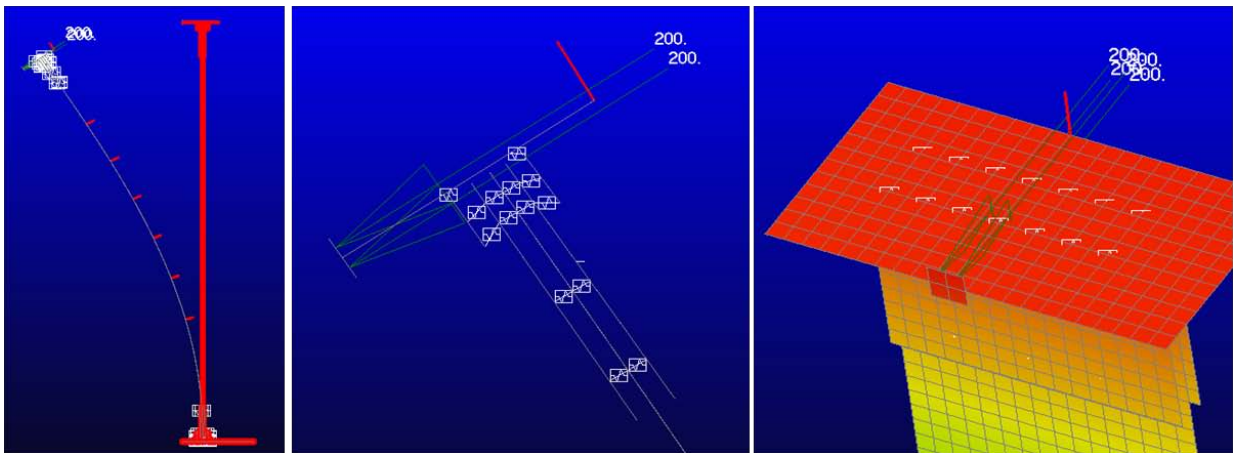

(a) (b) (c)

Figure 3.32: Follower-Force on Qualification FE model (a) Side View, (b) Top Mounting Structure Side View, and (c) Top Mounting Structure Isometric View

The follower-force was applied to the FEMs by applying a pressure load to a square section, shown in Figure 3.32(c) for the qualification FE model, which has an area of one square inch and is made up of four elements. The solutions for all of the load cases were computed using Nastran's nonlinear solver (SOL 106) with LGDISP=1. The use of nonlinear solver is necessary due to the large deformations involved in both test articles as well as the bend-twist coupling that occurs as result of the geometry of the joined-wing test article.

3.9 Correlating the Analytical and Experimental Results

In order to correlate the experimental and analytical data sets, the coordinates of the points of interests were zeroed with respect to one of the corners of the base plates. When the unloaded measurements of the test article were plotted on the same graph as the corresponding FEA model node locations, it was discovered that the data sets did not have the same coordinates with respect to the base plate corner. The differences are shown in Tables 3.1 and 3.2, and in Figures 3.33 and 3.34.

Table 3.1: Measurement Location Differences – Qualification Test Article vs. FEA Model

Data Point	Difference in Coordinate		
	X (in)	Y (in)	Z (in)
1	-1.2838	-0.2455	0.146
5	-1.0033	-0.1292	0.006
6	-1.0087	-0.1911	0.049
7	-0.8271	-0.0928	0.007
8	-0.8347	-0.1442	0.069
9	-0.6505	-0.0148	0.023
10	-0.6564	-0.1132	0.046
11	-0.4889	-0.0143	0.009
12	-0.4915	-0.0382	0.056
13	-0.3259	0.056	0.018
14	-0.3324	-0.0007	0.066
15	-0.1814	0.1194	0.011
16	-0.1814	0.0311	0.063

Table 3.2: Measurement Location Differences – Joined-Wing Test Article vs. FEA Model

Data Point	Difference in Coordinate		
	X (in)	Y (in)	Z (in)
Fore Wing Left Edge			
6	0.9879	0.2763	0.1314
8	0.4061	0.2158	0.1292
10	0.0424	0.1047	-0.0321
Fore Wing Right Edge			
7	0.9591	0.3114	0.0364
9	0.4275	0.3075	0.0032
11	0.0424	0.2088	-0.0491
Aft Wing Left Edge			
17	0.8442	0.1217	0.0567
19	0.006	-0.1131	0.1609
21	-0.5568	-0.3192	0.1046
Aft Wing Right Edge			
18	0.7788	0.1655	-0.0353
20	-0.0753	-0.0728	0.0889
22	-0.5724	-0.2679	0.1476

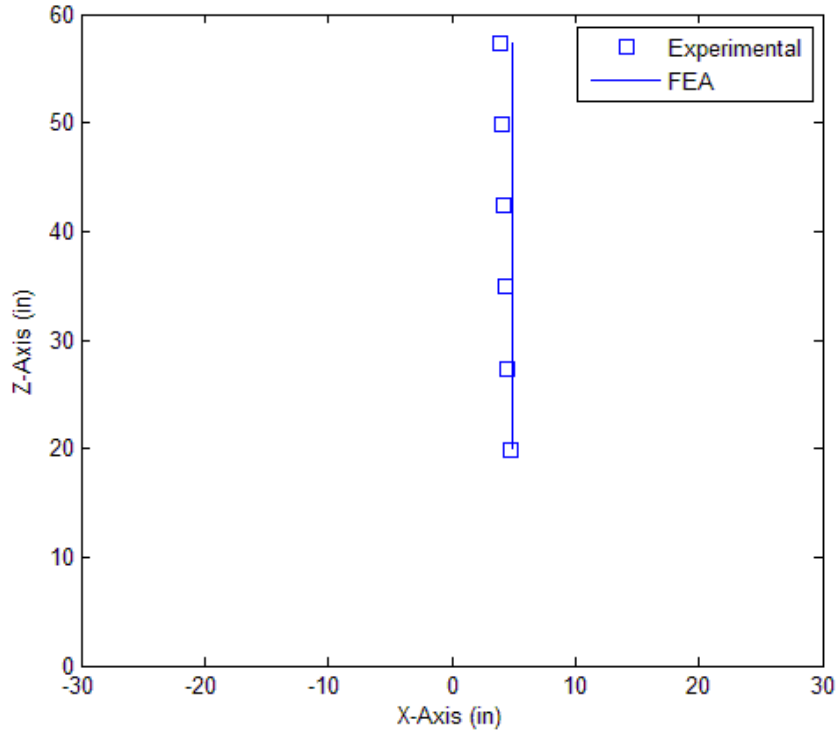

Figure 3.33: Unloaded Qualification Test Article vs. Unloaded FEA Model

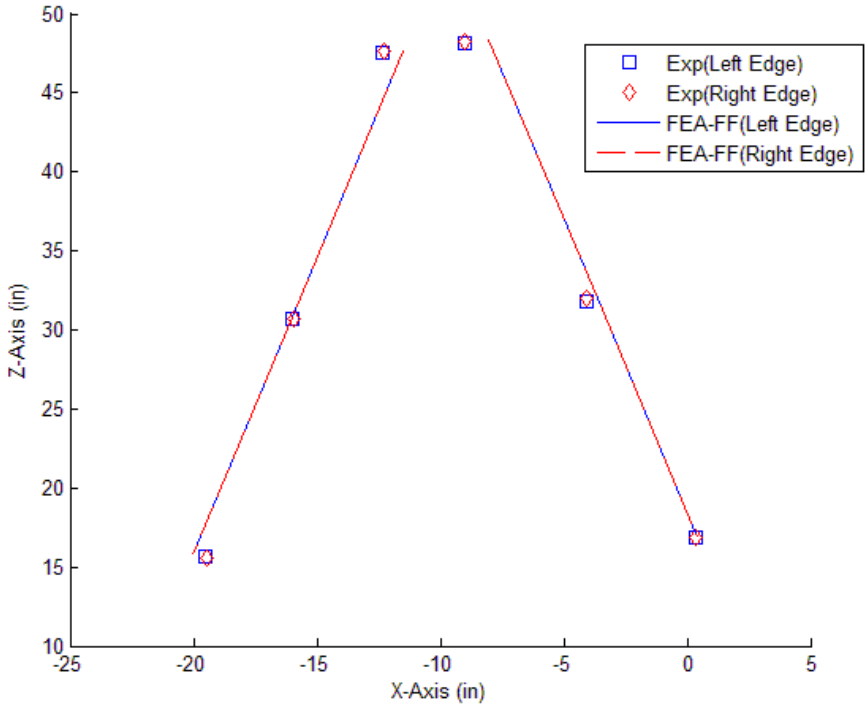

Figure 3.34: Unloaded Joined-Wing Test Article vs. Unloaded FEA Model

The differences found between the node positions of the qualification FEA model and the corresponding measurement points on the test article are most likely due to gravity. The qualification test article is found to be leaning over toward the load direction even when there is no load applied, which is probably due to the combination of unevenness of the ground and weight of the top mounting structure. The possible reasons for the differences between the joined-wing model and the test article include manufacturing tolerances on each of the components making up the test articles, small errors in the location of the base plates, and possible permanent deformations from the previous study in which the test articles were used. The comparison of the measurements between the two corners of the base plates for both the experimental and FEA data revealed that the actual base plates are about 0.5 in closer in the X-direction and about 0.5 in further apart in the Y-direction. This difference along with manufacturing tolerances and unevenness of the lab floor most likely made the largest contributions to the differences found in the measurement locations of the FEA models and the actual test articles for the unloaded case. Also, even though strains were monitored at the predicted high stress areas of the test articles to prevent permanent deformations, it is still possible that the test articles were damaged during the previous study or even during this study.

Regardless of the causes for the slight differences in the locations of the points of interest, since the actual locations cannot be directly compared, the displacements of the points will used. The comparisons are made between the experimental data collected and the analytical results obtained from the FEA using both follower and stationary direction forces.

3.10 Comparison to Previous Study

Unfortunately, the measurement points (see Figure 3.15) on the test articles from this study (with the exception of point 1 on the joined-wing test article) do not match the locations that Boston used in his study. However, since Boston was able to closely match his experimental data to his nonlinear FEA results, it should be possible to make an indirect comparison to Boston's data by comparing the experimental data from this study to Boston's FEA results. This is very convenient since nodes corresponding to the measurement points from this study can be created in the FEM to make the comparison to the previous study possible. The stationary direction force FEA results from the un-tuned FEMs in Section 4 are FEA results from Boston's study.

It should be noted that the type of load that Boston used in his experiment was a fixed point force load, while the type of load he used for his FEA results was a stationary direction force load (see Figure

3.18). The reason why two different types of loads were used was probably because his load application structure was not capable of applying a stationary direction force and because it is difficult to apply the fixed point force load in FEA. However, for small deformations of the test article, the direction of the fixed point force and stationary direction force loads should not be very different and therefore should cause similar deformations.

4. Results

The experiments were conducted on the qualification and the joined-wing test articles, and displacement measurements were collected using the laser tracker. The experimental data are compared to the follower and the stationary direction force results from FEA and some of the experimental data from the previous study by Boston[2].

4.1 Qualification Test Article

4.1.1 Incremental Loads – Qualification Test Article

The measurement locations on the qualification test article are shown in Figure 4.1.

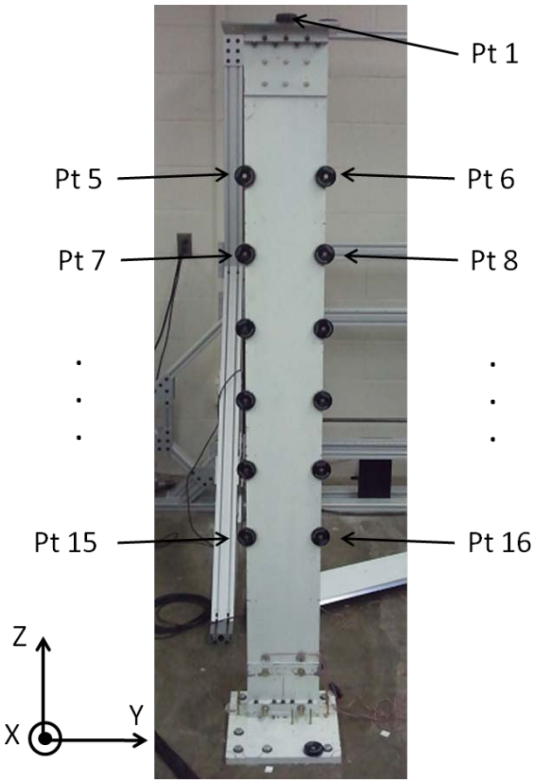

Figure 4.1: Tracker Measurement Locations

The experimental data from this research were collected using the method outlined in Section 3 and are used for comparisons against follower and stationary direction force FEA results. The stationary direction FEA results are from Boston's study and they represent his experimental data. The follower-force FEA results were obtained by applying a follower force to Boston's FEMs without making any modification to their properties.

Prior to comparison with the experimental data, the follower and stationary direction force FEA results are compared to determine if follower-force loads produce a noticeably different effect on the FEA predictions. As shown in Table 4.1, there are noticeable differences between the displacements predicted for the FEA models under follower and stationary direction forces. The positive values in the table indicate that displacements are greater under follower-force loads. As expected, the follower-force loads are predicted to cause the qualification model to bend over more about the Y-axis, which is seen indirectly by noting that there are greater displacements in the X- and Z-directions under follower-force loads. It is shown in Table 4.1 that the differences in displacements tend to increase with increasing load, and this difference is mostly likely due to the fixed orientation of the stationary direction load. The stationary direction force in FEA is always directed along the negative X-axis and as a result there is a component of the force that tends to pull on the model as the orientation of the model changes with deformation. Increasing the load causes the model to deform even more and the component of the load that pulls on the model increases while the component that causes the model to bend decreases (see Figure 4.2). This is probably why the largest percentage differences are in the vertical direction with about 13% difference in the displacements predicted for 200 lbs loads.

Table 4.1: Displacement Comparison – Follower vs. Stationary Direction Force Qualification FEA, Pt 1

Load	X	Y	Z	Total
25	0.52%	0.00%	0.21%	0.52%
50	1.23%	0.00%	4.78%	1.23%
75	2.00%	0.00%	7.48%	2.01%
100	2.77%	0.00%	8.17%	2.79%
125	3.51%	0.00%	9.40%	3.54%
150	4.21%	0.00%	10.72%	4.26%
175	4.88%	0.00%	12.05%	4.97%
200	5.53%	2.78%	13.35%	5.66%

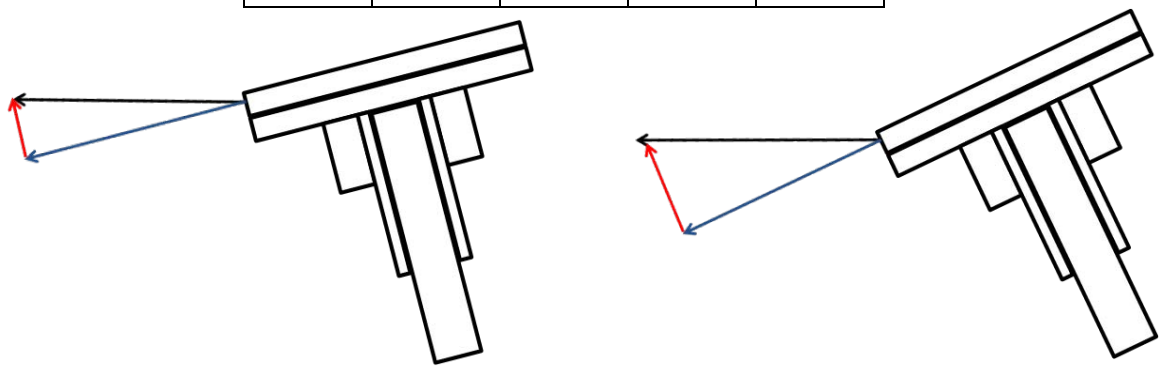

(a) (b)

Figure 4.2: Components of the Non-Follower Force for (a) Lesser and (b) Greater Loads

The data collected from the qualification test article under 200 lbs of follower-force load is plotted along with the corresponding FEA results in Figure 4.3. The data plotted are the measurement points from the left edge of the qualification model. The squares represent the experimental data, the solid line represents the follower-force FEA results, and the dotted line represents the stationary direction force FEA results. The graph clearly shows a large discrepancy between the experimental and the FEA results. It is expected that follower force loads will yield different results than the fixed point force applied by Boston in his study (represented by stationary direction FEA results), but the differences between the experimental and FEA follower-force results are a little puzzling since Boston[2] was able to closely match his experimental and FEA results. Since the same test article and FEA models were used for the current research it was expected that the experimental data and FEA predictions would match closely as it did in Boston's study.

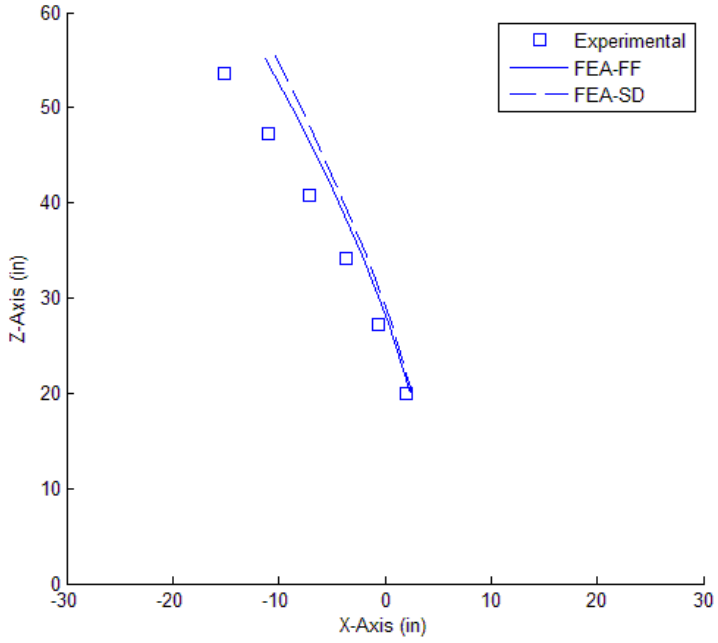

Figure 4.3: Deformed Shape under 200 lbs – Qualification Test Article

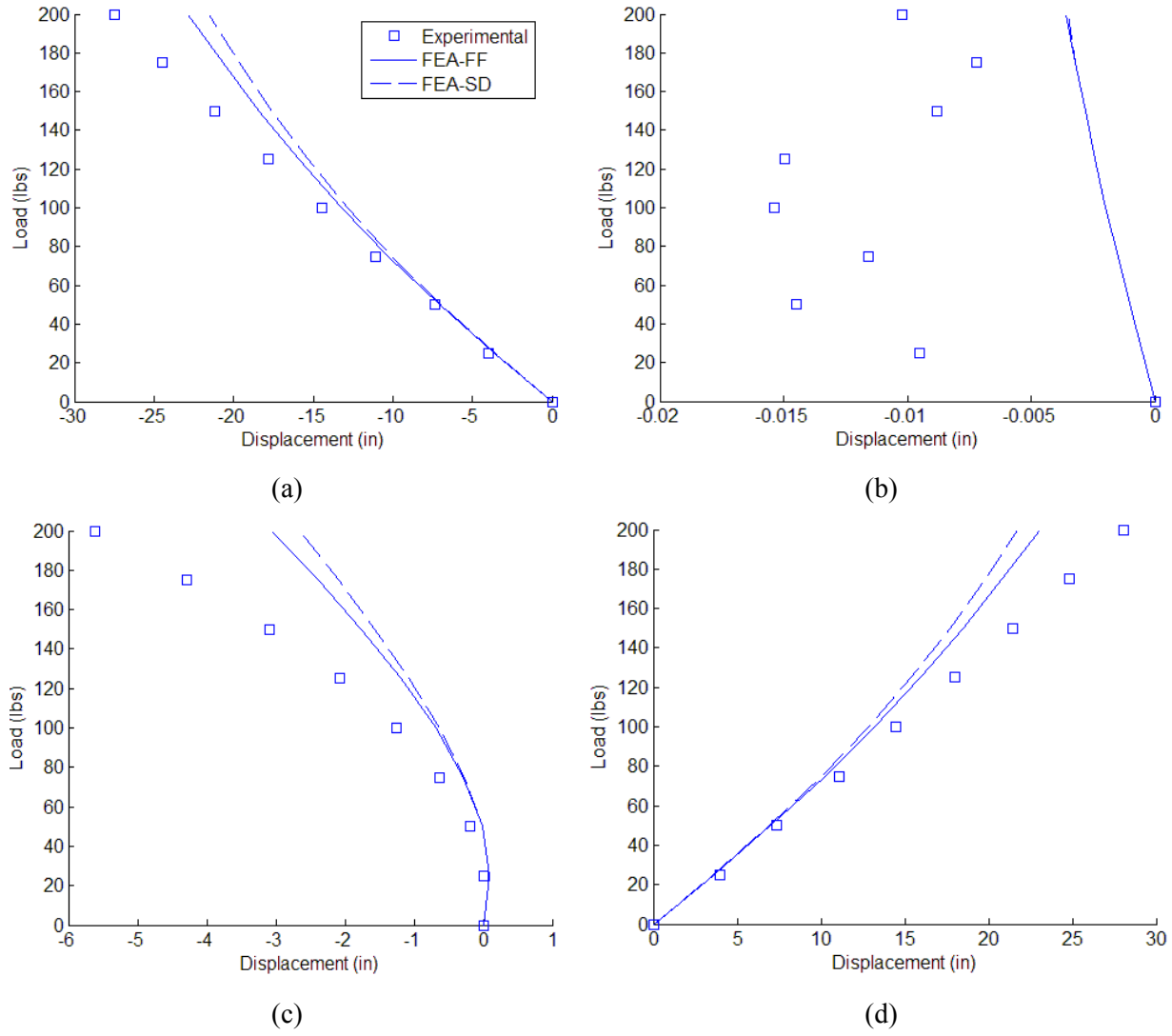

Figure 4.4: Displacement Comparison – Qualification Test Article Pt 1 (a) X-Axis (b) Y-Axis (c) Z-Axis and (d) Total Displacement

Table 4.2: Displacement Comparison – Qualification Test Article Pt 1

Load	Exp vs. FEA-FF (% Difference)			Exp vs. FEA-SD (% Difference)		
	X	Z	Total	X	Z	Total
25	9.96%	1493.33%	9.92%	10.42%	1490.00%	10.39%
50	4.20%	94.66%	4.23%	5.38%	96.84%	5.41%
75	7.31%	55.11%	7.43%	9.17%	58.47%	9.29%
100	8.66%	44.95%	8.87%	11.19%	49.45%	11.41%
125	10.90%	42.67%	11.25%	14.02%	48.06%	14.39%
150	13.27%	43.13%	13.78%	16.92%	49.22%	17.46%
175	15.36%	44.46%	16.08%	19.49%	51.15%	20.25%
200	16.89%	45.63%	17.85%	21.48%	52.89%	22.50%

The comparison of the displacements of point 1 is shown in Figure 4.4 and in Table 4.2. The figure and the table show comparisons in the X-, Y-, and Z-directions in addition to the total displacement. Point 1 is the furthest away from the base plate and shows the largest discrepancy to the displacement values predicted by FEA.

The general trends and shape of the graphs are similar, except for those in the Y-direction. The displacements in the Y-direction seem to be random, but given the absolute value of the displacements and their relative magnitude to the displacements in other directions, the test article essentially does not move in this direction. This is the expected result since the load direction was only changed in the XZ plane, and the small movements in the Y-axis direction shown in the measurements are due to 1 degree tolerance allowed for the load angle.

Overall, the experimental data shows larger displacements than those predicted by both follower and stationary direction force FEA results, which seems to indicate that the FEA model is stiffer than the actual test article. The largest differences are in the Z-direction with the percent differences being roughly 40% and 50% for follower and non-follower FEA results, respectively, when compared to the experimental data. Although the follower-force FEA results show slightly better agreement with the experimental data, the match between FEA and experiment was nowhere as close as that reported by Boston. The largest total displacement for the experiment is 28.04 in (38.95% of overall length of 72 in) at point 1, and the corresponding displacements for follower and stationary direction force results are 23.04 and 21.73 in, respectively.

Strain was monitored throughout the experiments to ensure that it never went above 4000 microstrain to prevent yielding of the test article. The yield limit determined by Boston was about 4500 microstrain, but he did not go above 4000 microstrain to give himself some cushion. The same guideline was used in the current research, and the strain readings are shown in Figure 4.5 along with those from Boston's experiments, which are shown as solid lines. The figure shows that max strain on the test article was just below 4000 microstain, and that the strain on the test article under follower-force load was higher, which corresponds to the larger deformations of the test article resulting from the follower-force loads.

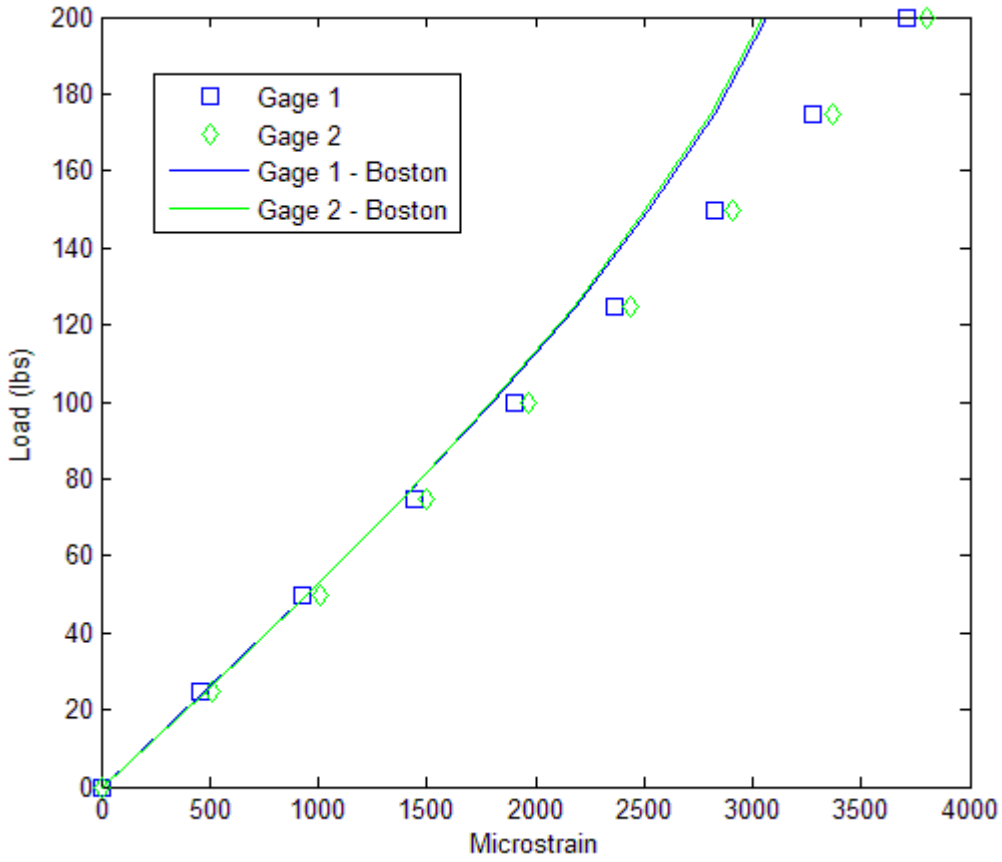

Figure 4.5: Strain vs. Load – Qualification Test Article

4.1.2 Direct Loads – Qualification Test Article

In order to determine if loading the test article directly to a high load will yield different results, the qualification test article was directly loaded to 125 lbs, 150 lbs, 175 lbs, and 200 lbs. Three sets of data were collected for each load and those data were compared to the data obtained from incrementally loading the qualification test article. The result is shown in Figure 4.6 and Table 4.3, where the data set that was closest to the incrementally loaded data set is highlighted in bold. The figure shows that the most of the data points for the direct loaded cases are within 0.3 in of the data for the incrementally loaded case. The largest difference occurs at point 1 under 125 lbs of load. Since point 1 has a total displacement of 17.96 in when incremental loaded to 125 lbs, the difference of 0.3 in as a percentage of the total displacement is only about 1.6%. This difference seems small enough conclude that incremental and non-incremental loading of the test article will yield the same result.

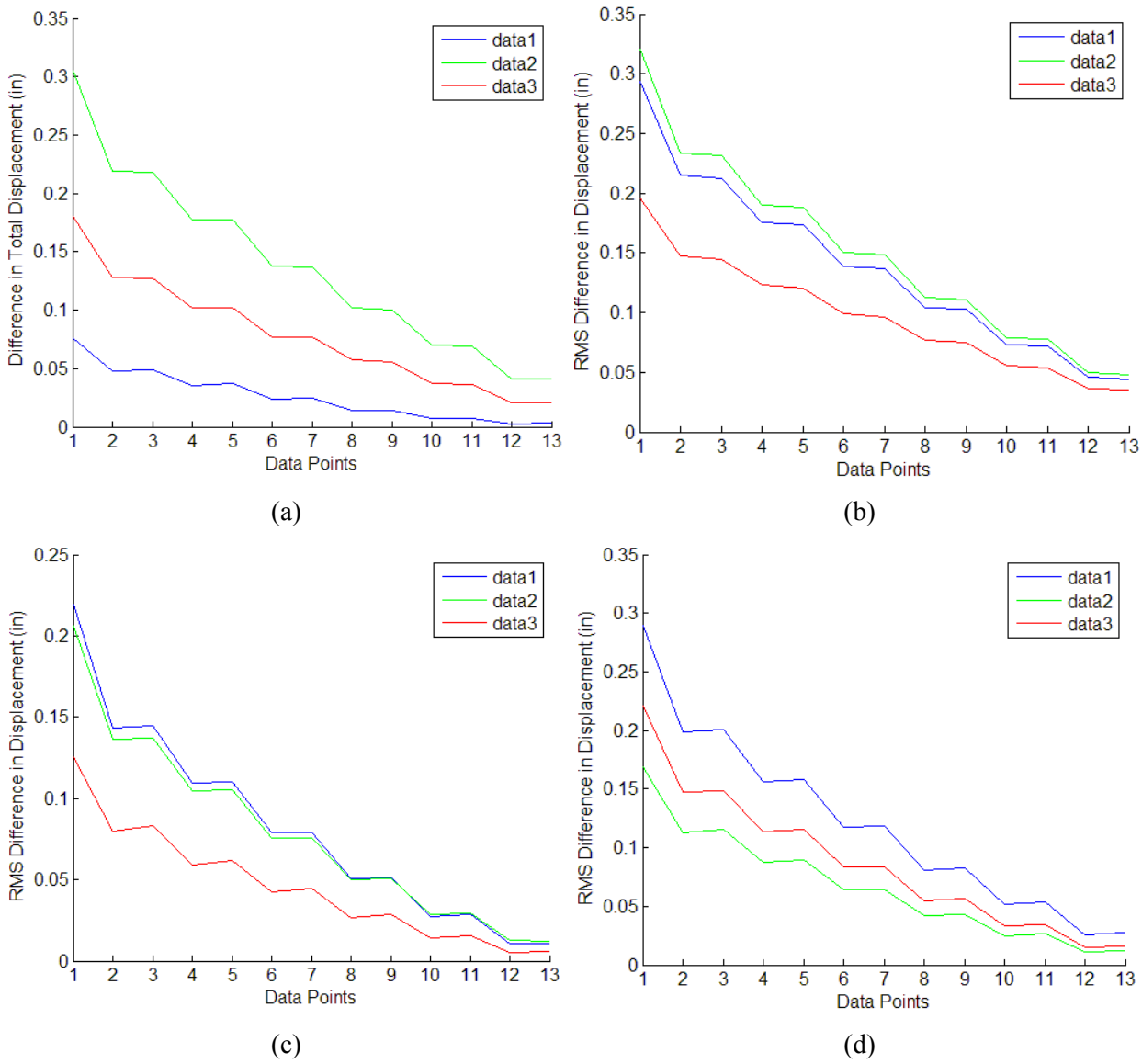

Figure 4.6: Displacement Comparison – Incremental vs. Direct Load (a) 125 lbs (b) 150 lbs (c) 175 lbs and (d) 200 lbs

The load angles shown in Table 4.3 do not seems to indicate that closeness of the load angle values indicate better correlation between the results. It seems logical that the data sets with relatively close load angles will have better matching data, but this is not true with the exception of the data for 125 lbs. However, since the load angles are measurements of the angle between the follower-force and actual load directions using the dot product, it does not take in account where the actual load direction is with respect to the desired direction. Therefore, even if the calculated values of angle obtained from dot products are close, the actual load directions for those angles may lie on either side of the follower-force direction. If this is the case, the data sets with load angles that are close in magnitude will not necessarily

be closely correlated. It is possible that the bolded data sets in the table show close correlation to the incremental case because their load directions are closer to the load direction in the incremental load case than others.

Table 4.3: Load Angle – Qualification Test Article, Direct Loads

Data Set	Load Angle (degs)			
	125 lbs	150 lbs	175 lbs	200 lbs
Direct 1	**0.2348**	0.6786	0.4230	0.4552
Direct 2	0.4814	0.3647	0.4375	**0.4785**
Direct 3	0.0953	**0.1118**	**0.4905**	0.4807
Increment	0.2542	0.3381	0.2753	0.2409

In the worst case, the load angles for the incremental and direct load cases could be on the opposite of the desired load direction so that the angle between them is 2 degrees, see Figure 4.7. In such a case the direct load force can be thought of as being composed of a component of the force in the direction of the incremental load direction and a component perpendicular to that direction. For a 125 lbs load the magnitude of the perpendicular component is 4.36 lbs if the angle between the two directions is 2 degrees. I f the angle between the two directions is 1 degree, the magnitude of the perpendicular component is 2.18 lbs. Although 2.18 lbs is not a large amount of force, given the flexible nature of the qualification test article it seems possible that such a sm all amount of force could account for the differences in displacements of about 0.3 in.

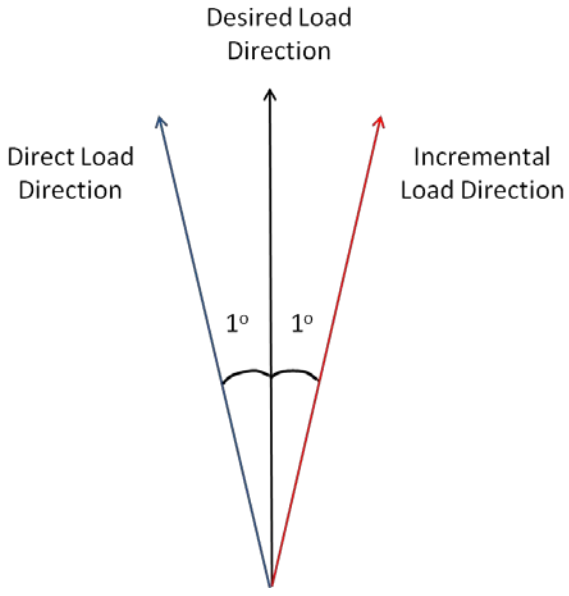

Figure 4.7: Variance in Load Direction

4.2 Joined-Wing Test Article

4.2.1 Incremental Loads – Joined-Wing Test Article

The experimental procedures, as described in Section 3, for the joined-wing test article are similar to the ones used for testing the qualification test article. The measurements points on the test article are shown in Figure 4.8.

Displacement data were collected using the laser tracker and the strain data was monitored to ensure that permanent deformations did not take place. The coordinate system is same as that used for the qualification test article, where the X-axis is opposite of the initial follower-force direction, the Z-axis is the vertical direction, and the Y-axis makes up the right-handed coordinate system.

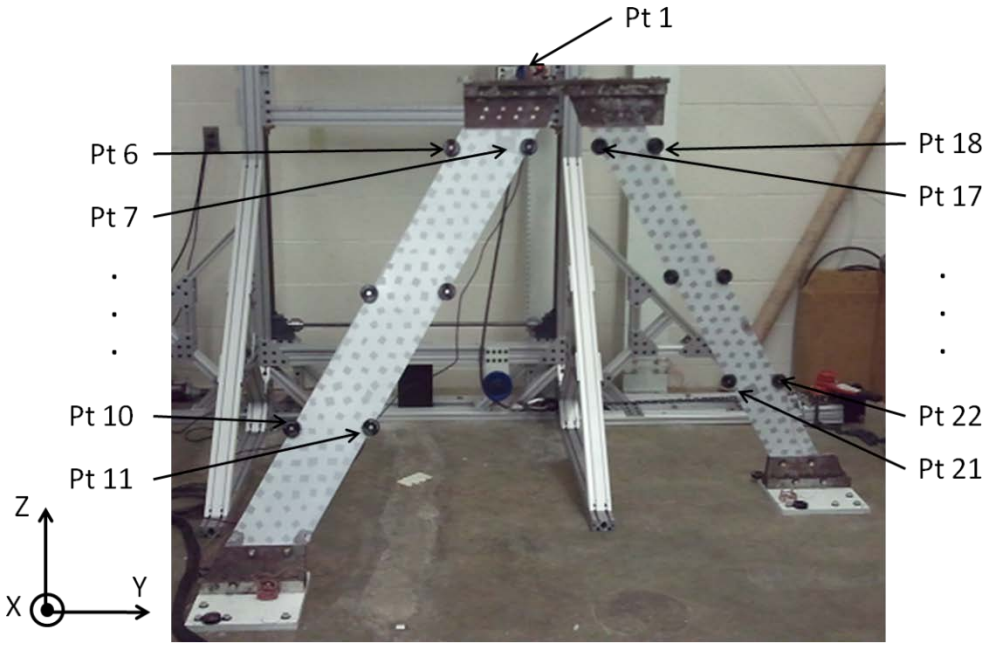

Figure 4.8: Tracker Measurement Locations – Joined-Wing Test Article

Table 4.4 shows a comparison of the follower and stationary direction force FEA results for point 1. The stationary direction force FEA results are representative of Boston's experimental data for the joined-wing test article. The positive values in the Table 4.4 indicate that the displacements are greater under follower-force loads. It is shown that the largest differences are in the Z-direction, which is similar to the result found when the follower and stationary direction force FEA predictions for the qualification

models were compared against one another. In the stationary direction force FEA case, the applied force on the joined-wing model can be thought of as consisting of two components. One of the components points roughly along the follower-force direction and the other component is normal to that direction. The normal component has the tendency to pull up on the joined-wing model and to counteract the deformation being caused by the follower-force component as discussed in Section 4.1.1. As a result, the joined-wing model deforms less when a stationary direction force is applied and the biggest differences in displacements, when compared to the follower-force result, are shown to be in the Z-component of the displacement.

Similar to the trend found for the qualification model, the differences between the follower and non-follower force FEA results increases with increasing load. However, while the differences in the two FEA results for the qualification models seems to be increasing gradually in a linear manner, the differences in the FEA results for the joined-wing models increase exponentially. This is because the qualification model initially deforms linearly with respect to the applied load due to its simple geometry, while the joined-wing model behaves nonlinearly from the onset due to its configuration.

Another difference between the qualification and the joined-wing FEA results is that the differences in the displacement of the joined-wing model are much smaller than the differences predicted for the qualification model. According to Table 4.4, the difference in displacements between the follower and stationary direction force FEA results are less than 1% until an 800 lbs load is applied to the model. The addition of the aft wing to the fore wing increases the stiffness of the structure so greatly that even when 800 lbs load is applied the joined-wing model deforms only about 3 in at the tip. The unit vector for the follower-force direction at for 800 lbs load is (-0.9964, 0.0235, -0.0813). Since the stationary direction force load is applied along the negative X-axis, it is easy to see that the follower and stationary diretion forces are essentially the same, and the small difference found in the resulting displacements are understandable. When an 1100 lbs follower-force is applied, the direction of the load is given by the unit vector (-0.9866, 0.0490, -0.1557), which shows why there is a greater difference between the two FEA results especially in the Z-axis direction.

Table 4.4: Displacement Comparison – Follower vs. Stationary Direction Force Joined-Wing FEA, Pt 1

Load	X	Y	Z	Total
25	0.01%	0.01%	0.05%	0.01%
100	0.05%	0.02%	0.21%	0.05%
200	0.11%	0.03%	0.32%	0.10%
300	0.17%	0.05%	0.36%	0.16%
400	0.25%	0.08%	0.33%	0.23%
500	0.36%	0.11%	0.23%	0.33%
600	0.50%	0.16%	0.02%	0.46%
700	0.71%	0.24%	0.37%	0.66%
800	1.07%	0.39%	1.11%	1.00%
900	1.74%	0.70%	2.63%	1.64%
1000	3.16%	1.41%	5.96%	3.01%
1100	6.26%	3.13%	12.88%	6.04%

In Figure 4.9 the shape of the joined-wing test article is shown when an 1100 lbs follower-force is applied to it. The experimental data are shown as squares (fore wing) and diamonds (aft wing), and the follower-force FEA data is shown as solid lines. The color blue is used for the left edges of the wings and the color red is used for the right edges of the wings. The figure shows a large difference between the predicted and measured displacements in addition to the bend-twist coupling response found in both the FEA model and the test article. Although it is not obvious at first glance, the twist in the joined-wing can be seen by comparing the X-axis values for the measured points, which shows that the bottom of the left edges of both the fore and aft wing are displaced less than the right edge while the opposite is true at the wing tips where the two wings are joined. The large differences in the measured and predicted displacements suggest that the current FEA model cannot be directly used to predict the behavior of the joined-wing test article when a follower-force load is applied.

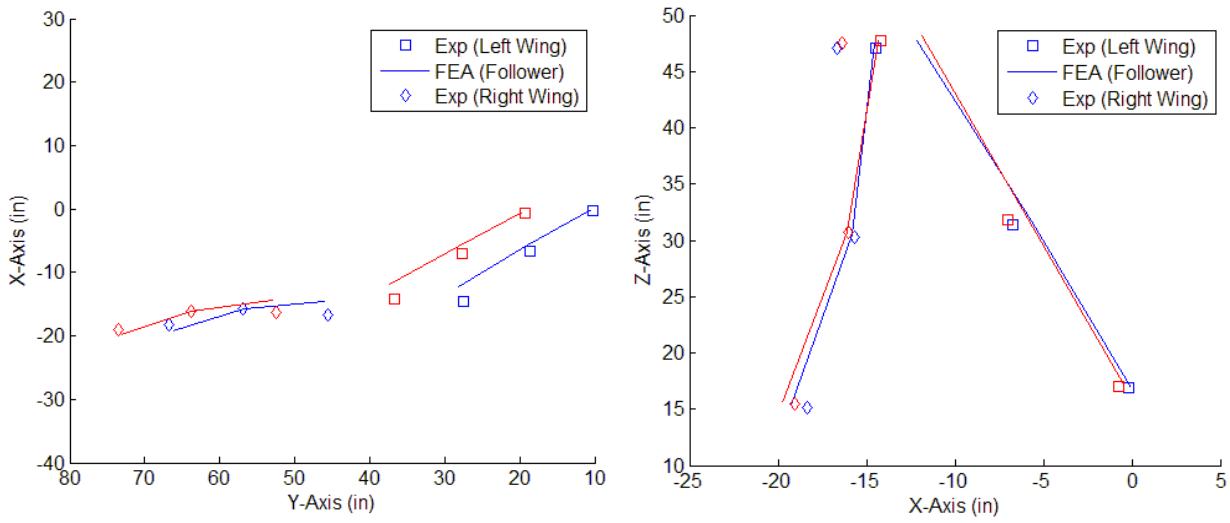

(a) (b)

Figure 4.9: Deformed Shaped under 1100 lbs – Joined-Wing Test Article (a) in the XY Plane and (b) in the XZ Plane

The comparison of the displacements of point 1 is shown in Figure 4.10 and Table 4.5, where displacements in the X-, Y-, and Z-axis directions in addition to the total displacement are compared. Point 1 is located farthest away from the base plates and displays the largest discrepancy to the displacement values predicted by FEA.

It is evident from the general trends shown in Figure 4.10 that FEA is able to accurately capture the overall response of the joined-wing test article. Overall, the experimental data collected from the joined-wing test article seems to match the FEA predictions better than the data collected from the qualification test article. This is especially true for the displacements in the X- and Y-axis directions where the deviations were below or at about 10% for loads up to 800 lbs. The reason for the good match can probably be attributed to the stiffness of the joined-wing test article. Due to its stiffness, the test article does not deform much at loads below 800 lbs and even when loaded at 800 lbs the total displacement of point 1 is only 3.36 in, which is about 46% of the total displacement of 7.36 in at 1100 lbs load. As a result, the direction of the forces applied to the test article, both follower and stationary direction forces, up to about 800 lbs are not very different. The largest difference between the direction of the follower and non-follower force loads is in the Z-direction. The follower-force tends to point down as the test article deforms, while the stationary direction force maintains its original direction even as the test article deforms. However, the magnitude of the Z-components of the follower-force loads is relatively small in comparison to the horizontal component, even at 800 lbs. Since the majority of the applied loads are in the horizontal direction, it makes sense that the reactions of the test article are similar.

The displacements in the Z-axis direction show the largest discrepancy when compared to the FEA predictions. A part of the reason why there are large differences in displacements is because of the differences in the vertical components of the follower and stationary direction force loads as mentioned above. This would explain why the displacements are different between the experimental data and the non-follower force FEA predictions. The follower-force load tends to pull the test article down, while the non-follower force load tends to pull the test article up.

The other reason for the differences between experimental data and FEA predictions is that the FEA model may have been tuned to be too stiff, which would explain why the joined-wing FEA model deforms less for a given follower-force load. This would explain the difference seen between the experimental data and the follower-force FEA predictions.

Although both of the FEA results predict the test article to be stiffer than the experimental data suggests, the follower-force FEA results are shown to be a slightly closer match to the actual data. Comparison of the percent difference between the FEA and experimental results show that the displacements in the X-axis direction have the best correlation and that the displacements in the Z-axis direction have the worst correlation. The largest displacement for point 1 during the experiment was 7.36 in, and the corresponding values from follower and non-follower force FEA being 5.42 in and 5.09 in, respectively, which correspond to percent differences of 26.35% and 30.80% as shown in Table 4.5.

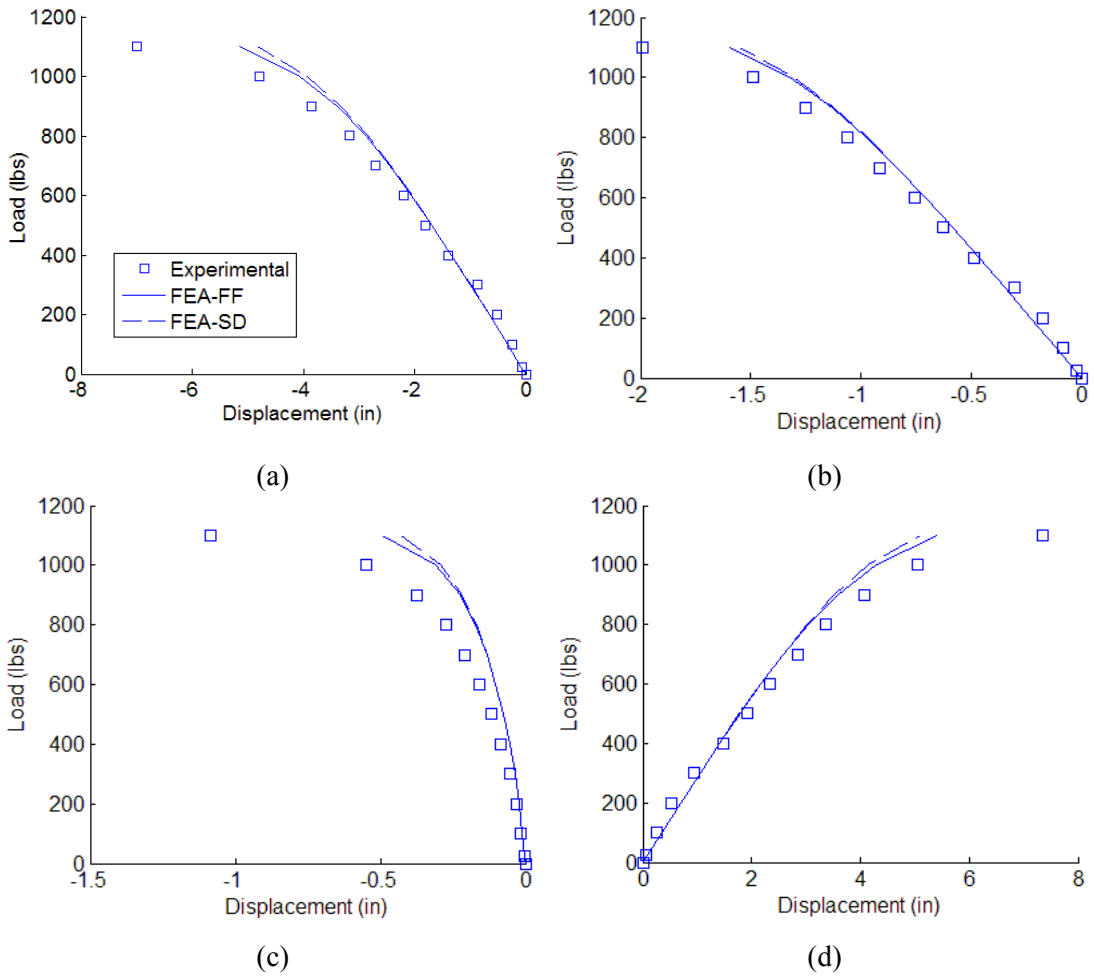

Figure 4.10: Displacement Comparison – Joined-Wing Test Article Pt 1 (a) X-Axis (b) Y-Axis (c) Z-Axis and (d) Total Displacement

Table 4.5: Displacement Comparison – Joined-Wing Test Article Pt 1

Load	Exp vs. FEA-FF (% Difference)				Exp vs. FEA-SD (% Difference)			
	X	Y	Z	Total	X	Y	Z	Total
100	34.83%	41.01%	33.24%	35.32%	34.76%	40.99%	33.11%	35.25%
200	30.20%	34.11%	28.44%	30.46%	30.06%	34.06%	28.21%	30.34%
300	13.50%	15.00%	28.58%	13.55%	13.30%	14.94%	28.32%	13.37%
400	3.91%	4.58%	36.75%	4.08%	4.16%	4.65%	36.54%	4.30%
500	6.27%	6.88%	36.37%	6.44%	6.61%	6.98%	36.23%	6.75%
600	6.30%	6.23%	35.22%	6.40%	6.76%	6.37%	35.21%	6.83%
700	9.21%	8.39%	37.00%	9.25%	9.86%	8.61%	37.24%	9.85%
800	9.51%	7.90%	37.16%	9.50%	10.48%	8.26%	37.86%	10.40%
900	12.27%	9.51%	40.38%	12.21%	13.80%	10.14%	41.94%	13.65%
1000	15.25%	11.24%	43.44%	15.17%	17.93%	12.49%	46.81%	17.73%
1100	26.36%	19.85%	54.52%	26.35%	30.97%	22.36%	60.38%	30.80%

To prevent yielding in the test article, strain values were recorded during the experiment as the load was being applied. The strain values recorded during the experiment are shown in Figure 4.11 along with the data from Boston's study, and the strain gage locations are shown in Figure 4.12. The maximum value of strain, 3627 microstrain, is found to be at the location of gage 3 under 1100 lbs load. Considering that the strain at 1000 lbs was 2636 microstrain, it was likely that the test article would have yielded before reaching 1200 lbs, so the experiment was stopped at 1100 lbs. It is seen from Figure 4.11 that higher strain is present in the test article when the follower-force is applied, which agrees with the observation that the test article deflects more under follower-force loads.

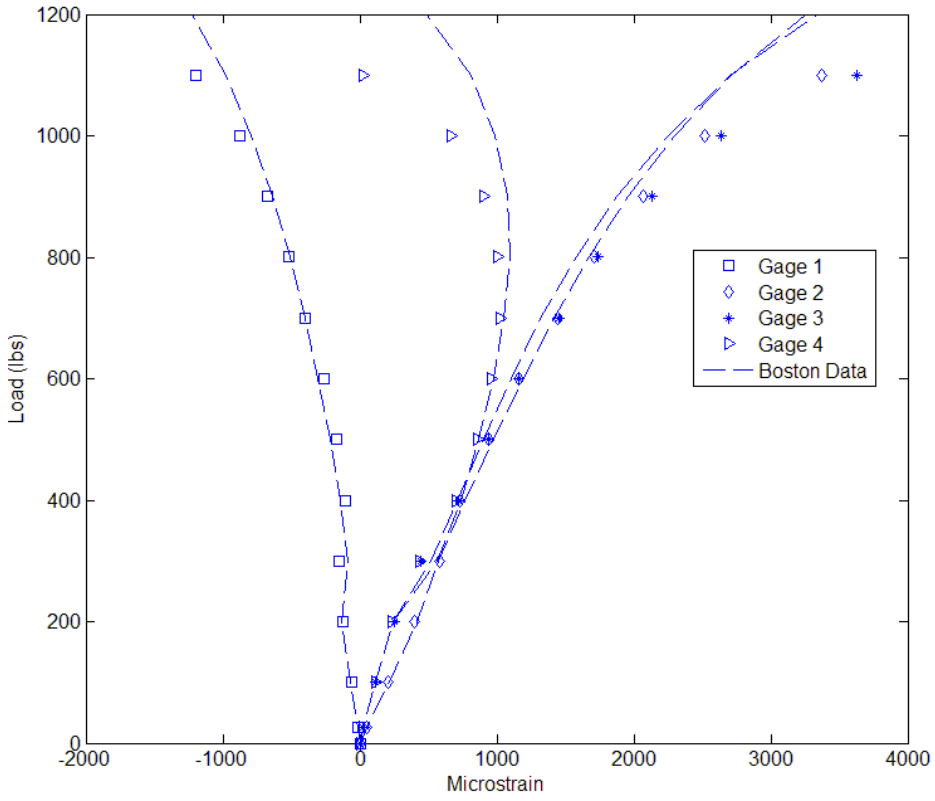

Figure 4.11: Strain vs. Load – Joined-Wing Test Article

Figure 4.12: Strain Gage Locations – Joined-Wing Test Article

4.2.2 Direct Loads – Joined-Wing Test Article

To determine whether loading the test article directly to a high load will yield different results, the joined-wing test article was loaded directly to 1100 lbs after data collection on a set of incremental loads was completed. Since it was determined that incrementally or directly loading the test article to a given load does not seem make a difference in the resulting displacements for the qualification test article, it seemed likely that the same would be true for the joined-wing test article.

Two sets of data were collected after directly loading the joined-wing test article to 1100 lbs. The comparison of the displacements recorded for the direct and incremental loads is show in Figure 4.13, which shows that the biggest difference occurs at the tip of the joined-wing test article where points 1 through 4 are located. The difference observed at point 1 is around 0.4 in, which is about 5% of the total displacement of point 1 at 1100 lbs of load. Although the percent difference in the displacements is not as low as in the qualification test article case, 5% still seems low enough to conclude that the incremental or direct loading has no significant effect on the deformation of the test article.

The load angle for the incrementally loaded case was 0.60 deg, and the load angles for the directly loaded cases were 0.81 deg for data set 1 and 0.76 deg for data set 2. Figure 4.13, however, shows that there is better correlation between data set 1 of the directly loaded case and the incrementally loaded case. Although it would seem logical that data set 2 should have a better correlation with the data from obtained by incrementally loading the test article, since the actual orientation of the load direction is cannot be determined from the results of a dot product, it is not possible to determine how close two load cases are from one another with just the load angle. Therefore, even if there seems to be a larger

difference between the load angles for two given load cases, it is possible for them to be the pair that are closest to one another.

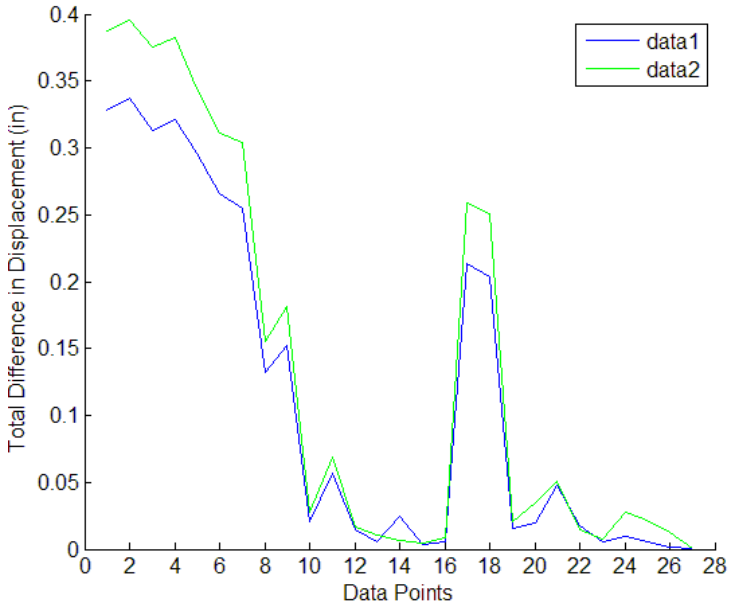

Figure 4.13: Displacement Comparison – Incremental vs. Direct Load on Joined-Wing Test Article

When two loads are compared, one of the loads could be thought of as being composed of two components with one component along the direction of the other load and one component perpendicular to the direction of the other load. The magnitude of the perpendicular component would increase as the angle between the two loads increases. If the angle between the two 1100 lbs loads is 1 degree, the magnitude of the perpendicular component of the force would be about 19.20 lbs. Considering that the displacement of point 1 on joined-wing test article between 1000 lbs and 1100 lbs loads is 0.73 inches in the YZ plane, it could be argued through simple algebra that 19.20 lbs would account for about 0.14 in. Although direction of the load has been ignored and the deflection of the test article has been assumed to be linearly proportional to the applied load for this quick comparison, it nonetheless seems likely that as much as two thirds of the difference shown in Figure 4.13 could be attributed to small differences in the direction of the load applied to the test article.

4.3 Discussion

It is evident that from the data presented so far that there is a large discrepancy between the FEA predictions and the follower-force experimental data. The difference was expected between the stationary direction force FEA predictions and the experimental data since the loads are applied in different

directions. However, since the FEA models were tuned already to match the results of the fixed point force (an approximation to the stationary direction force) experiments by Boston[2], a close correlation was expected for the follower-force experiments as well. This was not the case as already shown in previous sections, since there was a difference in tip displacement of about 5 and 2 in for the qualification and the joined-wing test articles, respectively.

One possible contributor to this difference could be the movement of the base plates. The rotation of the base plate was calculated to be 0.0026 radians or about 0.15 degrees for the qualification test article when loaded at 200 lbs. Assuming a length of 72 in, which is longer that the distance between the base plate to the tip of the deformed qualification test article, this equates to a displacement of about 0.19 in at the tip. For the joined-wing test article, the rotation of the base plates were found to be 0.0011 and 0.0016 radians, which equates to about 0.07 and 0.09 in of displacement due to rotation for a length of 57 in. The small amounts of rotation calculated for the base plates show that the assumption of fixed boundary conditions at the base plate was correct. It also shows that the large differences in displacements predicted by FEA and measured in the experiment cannot be due to the movement of the base plates.

Other possible cause of the differences could be due to some of the issues with the load application system. One of the issues encountered during the experiment was that the load cell would tend to rotate a little as the load increased, as shown in Figure 4.14. This was an issue only on the joined-wing test article with load in the excess of 500 lbs. Although, the load cell's orientation was corrected as much as possible using measurements of the eye, some error could have been introduced in the alignment of the applied force to the follower-force direction. Assuming that the load cell was rotated by 10 degrees from the normal orientation shown in Figure 4.14(a) and given that the distance from the middle of the load cell to the measurement point is 2.125 in, the error in the position of the measurement point is 0.37 in. Since the distance from point 4 and point 5 is about 9 in, the error in the load angle would be about 0.0411 radians or 2.36 degrees. It was shown in the previous section that an error of 1 degree in the load direction for the joined-wing test article may be responsible for about 0.14 in of displacement for a load of 1100 lbs, so an error of 2.36 degrees could be responsible for a difference in displacement of about 0.3 in. This is a little more substantial that the effects due to the base plate movements, but still does not account for the 2 in difference between the FEA predictions and the measured data for the joined-wing test article.

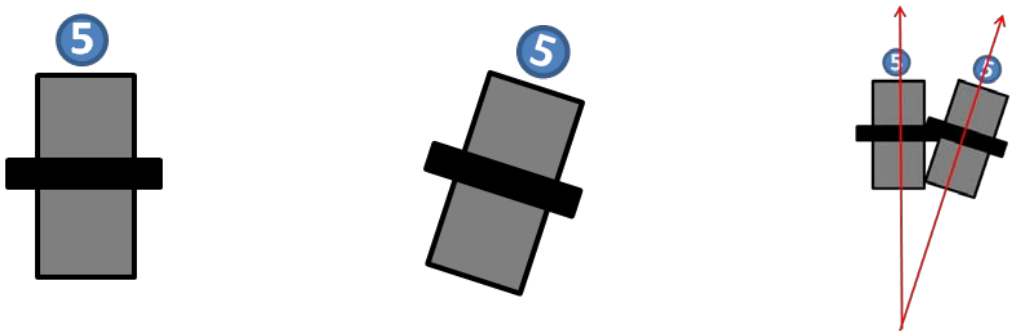

(a) (b) (c)

Figure 4.14: Load Cell Viewed Along the Direction of the Load (a) Normal Orientation (b) Rotated Orientaiton (c) Difference Due to Rotation

The second issue encountered with the load application system during the experiment is illustrated in Figure 4.15. Since the load cell is connected to the load cable using cast iron links, it was noticed that the direction of the load cable did not always align with the length of the load cell. The amount of misalignment would change how much the pulley would have to be moved on the load application system. However, this issue should not cause any errors in the load direction, since the load direction is determined solely from the measurements of points 1-5 on the joined-wing test article. So even though the kink in the link will cause some variance in the pulley position for the same follower-force loads applied to the test article, it will not result in errors of the load direction.

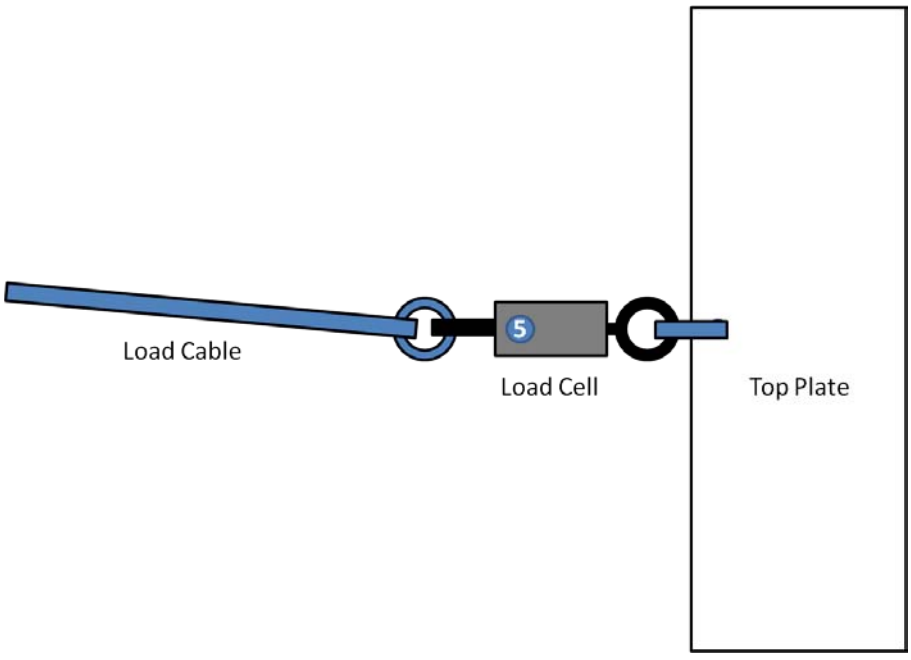

Figure 4.15: Test Article under Load – Top View

The most likely cause of the major differences between the measured data and the FEA predictions is the stiffness value used for the 6DOF springs in the FEA model. These springs are used to model the bolts which hold the test articles together and the deflections of the FEA models change based on the stiffness values used for the springs.

Boston[2] adjusted the stiffness of the FEA models until he obtained a close agreement between his experimental data and FEA predictions. However, the load that Boston applied to the test article, shown in Figure 4.16(a), is different from the load applied to the FEA model, shown in Figure 4.16(b). The stationary direction force can be broken into horizontal and vertical components, with the magnitude of vertical component increasing as the angle of the load from the horizontal direction increases. In terms of moments about the base plate, the vertical component of the load opposes the horizontal component. Therefore, for a given load the moment resulting from the experiment non-follower force will be less than the moment caused by the FEA non-follower force. The equivalent FEA non-follower forces that will cause the same moment about the base plate as the experiment non-follower forces for the qualification test article are shown in Table 4.6. The differences in the loads in Table 4.6 show that Boston tuned his FEA model to data obtained with loads less than those used for the FEA models.

This means that the qualification FEA model is stiffer in comparison to the qualification test article, and although the exact amount is unknown, some of the differences in the displacements between the FEA predictions and the measured data can be attributed to the differences in the loads. To determine the exact effects of this tuning problem, the data will have to be collected again on the qualification test article using the same loads that were applied to the FEA model or the 6DOF spring constants in the FEA model should be adjusted until the predictions for the equivalent loads in Table 4.6 match the measured data. Table 4.6, indicates that the difference between the experiment non-follower force and the FEA non-follower force is about 10 lbs for a 200 lbs load on the qualification test article.

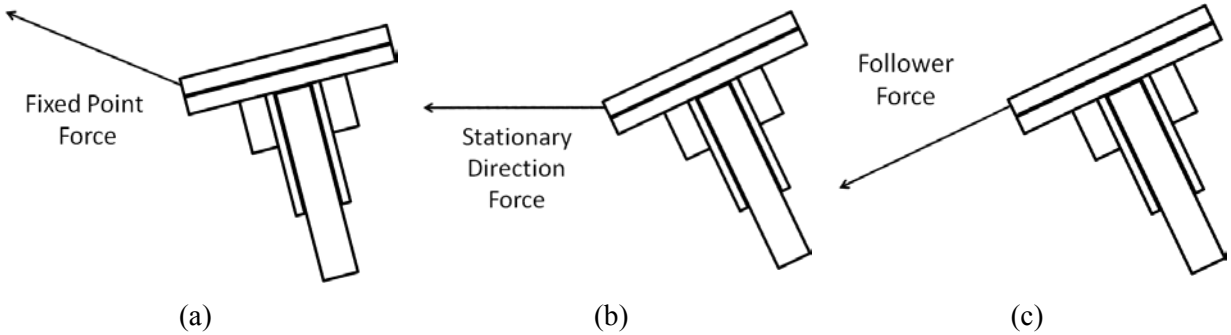

Figure 4.16: Applied Load Directions – (a) Boston's Experiment, (b) Non-Follower Force FEA, and (c) Current Experiment

Table 4.6: Equivalent FEA Non-Follower Force to the Experiment Stationary Direction Force – Qualification Test Article

Experiment Fixed Point Force	Equivalent FEA-SD Force
25	24.99
50	49.90
75	74.63
100	99.03
125	122.94
150	146.19
175	168.60
200	189.98

Also, considering that the X-axis direction displacement for point 1 on the qualification FEA model from 175 lbs to 200 lbs is 2.15 in, the difference of 10 lbs would account for a displacement of about 0.86 in. If the FEA model is tuned so that it is less stiff, then 10 lbs will cause a displacement greater than 0.86 in. Until the FEA model is re-tuned it's not possible to determine whether resolving the tuning issue will remove all of the discrepancies between the FEA predictions and the measured data, however, it is evident that this issue seems to be the biggest reason for the differences found.

One of the assumptions underlying this research is that the same experimental data would be collected if Boston's[2] experiment was repeated using the new load application system. This assumption was made since the same test articles were used for the current experiment at the exact location where Boston's experiments were conducted. However, based on the large differences between the FEA predictions and the measured data, it would be interesting to see whether the data collected using non-follower forces indeed matches Boston's data. If the two data sets match, much of the differences found between the measured data and FEA predictions could be attributed to the tuning issue mentioned above.

4.4 Re-tuning the FEMs

In order to achieve better agreement between the experimental data and the follower-force FEA results, the FEMs of the qualification and joined-wing test articles were re-tuned. The only changes made to the FEM were in the values of the 6DOF spring element stiffness. This was the process that Boston had to go through to get his FEA results to match his experimental data.

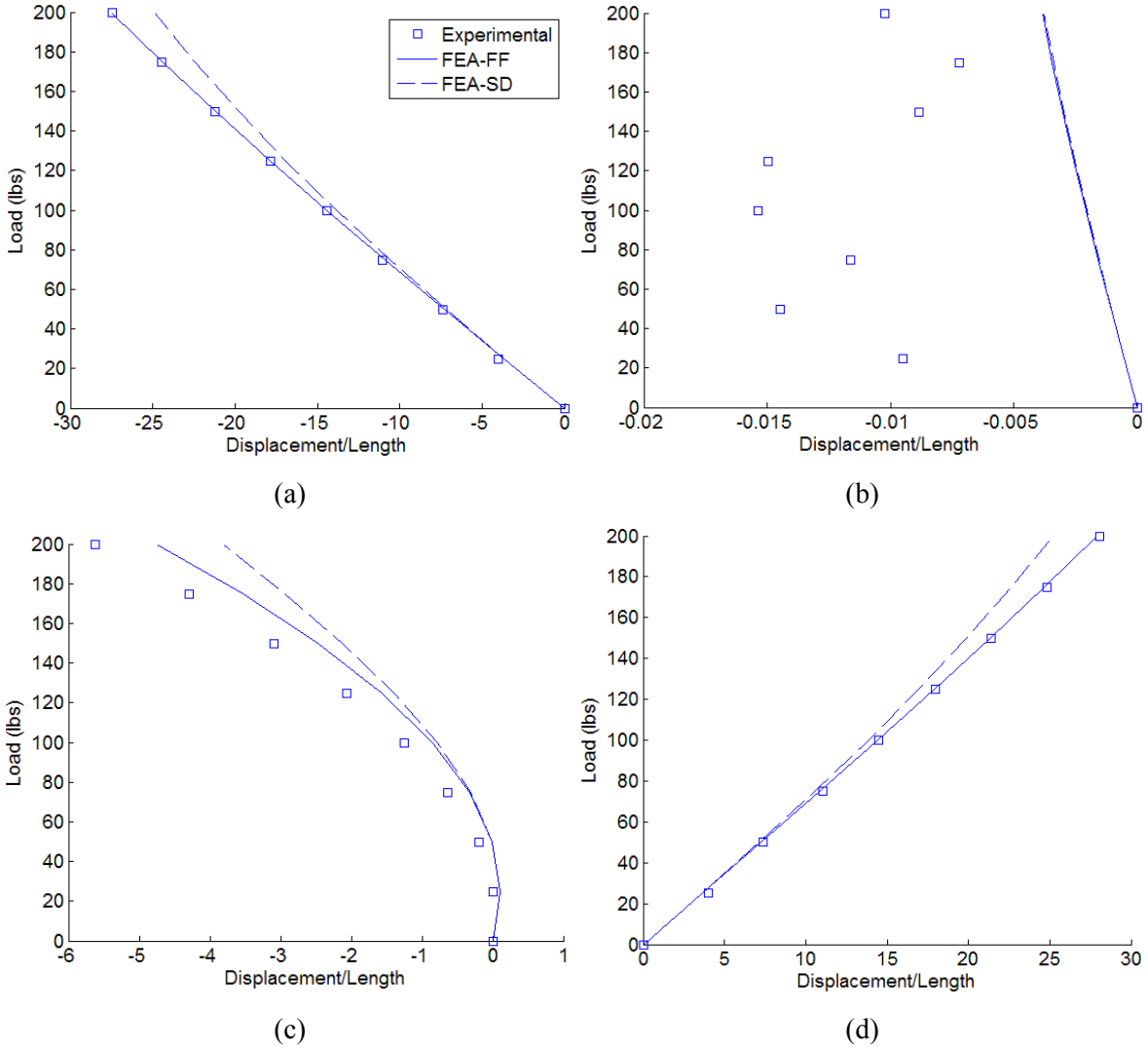

Figure 4.17: Displacement Comparison – Re-Tuned Qualification Test Article Pt 1 (a) X-Axis (b) Y-Axis (c) Z-Axis and (d) Total Displacement

Table 4.7: Displacement Comparison – Re-Tuned Qualification Test Article Pt 1

Load	Exp vs. FEA-FF (% Difference)			Exp vs. FEA-SD (% Difference)		
	X	Z	Total	X	Z	Total
25	8.78%	1657.53%	8.74%	9.33%	1621.43%	9.29%
50	1.10%	98.54%	1.13%	2.56%	97.38%	2.60%
75	1.79%	49.25%	1.91%	4.33%	51.47%	4.45%
100	0.41%	32.39%	0.61%	4.25%	37.57%	4.45%
125	0.06%	24.58%	0.35%	5.28%	32.71%	5.60%
150	0.11%	20.41%	0.49%	6.75%	31.46%	7.20%
175	0.17%	17.83%	0.66%	8.24%	31.77%	8.85%
200	0.09%	15.47%	0.49%	9.40%	32.36%	10.21%

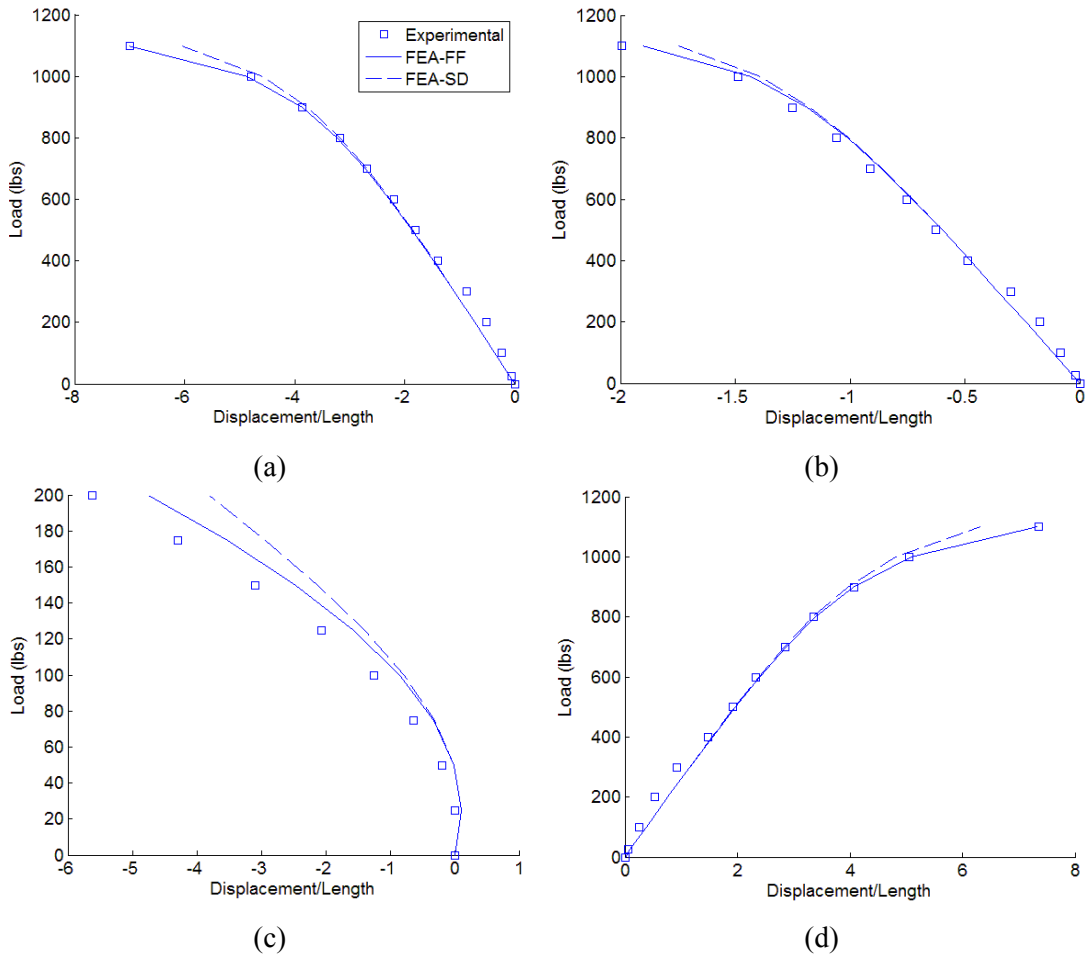

Figure 4.18: Displacement Comparison – Re-Tuned Joined-Wing Test Article Pt 1 (a) X-Axis (b) Y-Axis (c) Z-Axis and (d) Total Displacement

Table 4.8: Displacement Comparison – Re-Tuned Joined-Wing Test Article Pt 1

Load	Exp vs. FEA-FF (% Difference)				Exp vs. FEA-SD (% Difference)			
	X	Y	Z	Total	X	Y	Z	Total
100	48.28%	44.48%	20.08%	47.82%	48.17%	44.46%	20.12%	47.73%
200	43.21%	37.37%	23.18%	42.56%	43.00%	37.33%	23.21%	42.37%
300	24.90%	17.80%	18.65%	24.15%	24.61%	17.74%	18.63%	23.89%
400	5.84%	2.21%	2.02%	4.99%	5.49%	2.29%	1.89%	4.66%
500	3.41%	4.49%	0.10%	2.58%	2.92%	4.60%	0.20%	2.12%
600	3.67%	3.66%	0.23%	2.91%	2.97%	3.83%	0.82%	2.26%
700	0.92%	5.60%	4.62%	0.24%	0.08%	5.88%	5.67%	0.69%
800	1.47%	4.53%	5.89%	0.85%	0.11%	5.05%	7.85%	0.63%
900	0.21%	5.03%	10.30%	0.36%	2.54%	6.09%	14.20%	2.96%
1000	1.27%	3.96%	10.48%	0.69%	4.47%	6.57%	19.58%	4.81%
1100	0.18%	4.55%	11.91%	0.41%	13.72%	12.34%	34.05%	14.00%

After some trial and error it was discovered that only the top mounting structure spring element stiffness values had to be changed to have better agreement between the FEA results and the experimental results. The results after the re-turning are shown in Figure 4.17 and in Figure 4.18.

It is evident from these figures above that there is a much better agreement between the FEA results and the experimental data after the 6DOF spring elements in the top mounting structures were adjusted. For both the qualification and the joined-wing test articles, the follower-force FEA results lie almost on top of the experimental data for the X-direction displacements and the total displacements. Interestingly, for the joined-wing case there is a greater percentage difference between the follower-force FEA results and the experimental data in the Y-direction than in the X-direction, which is the reverse of the situation prior to the tuning of the spring elements. The largest differences between the FEA results and experimental data are still in the Z-direction, which seems to suggest that the FEA software may not be able to accurately model the follower-force behavior.

The good agreement between the follower-force FEA and experimental data after the tuning of the spring element seems to suggest that the FEA is providing valid results for the qualification and the joined-wing test article. However, because the FEMs which were tuned for a certain load type in the previous study had to be re-tuned for another type of load, there is some doubt as to whether the FEMs are truly accurate. It does not seem to be very logical that a model of a test article has to be adjusted for each type of load applied to it.

As a check to verify the validity of the FEMs, the qualification FEM was chosen to repeat the analysis of large deformations for a cantilever beam found in Gere and Timoshenko.[15] The qualification FEM was chosen for the validation because of its simple shape and likeness to a cantilever beam. The result of the analysis is shown in Figure 4.19.

It is not surprising that minor disagreements exist between the Gere and Timoshenko predictions and the measured displacements due to the addition of stiffening plates at each end of the test article. However, this close agreement between the FEA results and theoretical values suggests that the FEM of the qualification test article is providing valid results. Since the qualification FEM is providing results that match both the follower-force experiment data and theoretical predictions for large deformations of a cantilever beam, it seems likely that the re-tuned qualification FEM is accurate.

Due to the likelihood that the qualification FEM used in the previous study was inaccurate, it seems equally likely that there may have been some inaccuracies in the tuning of the joined-wing FEM as

well. Further study is required to validate the accuracy of the current re-tuned joined-wing FEM to ensure that it will give yet another erroneous result if a different type load is applied.

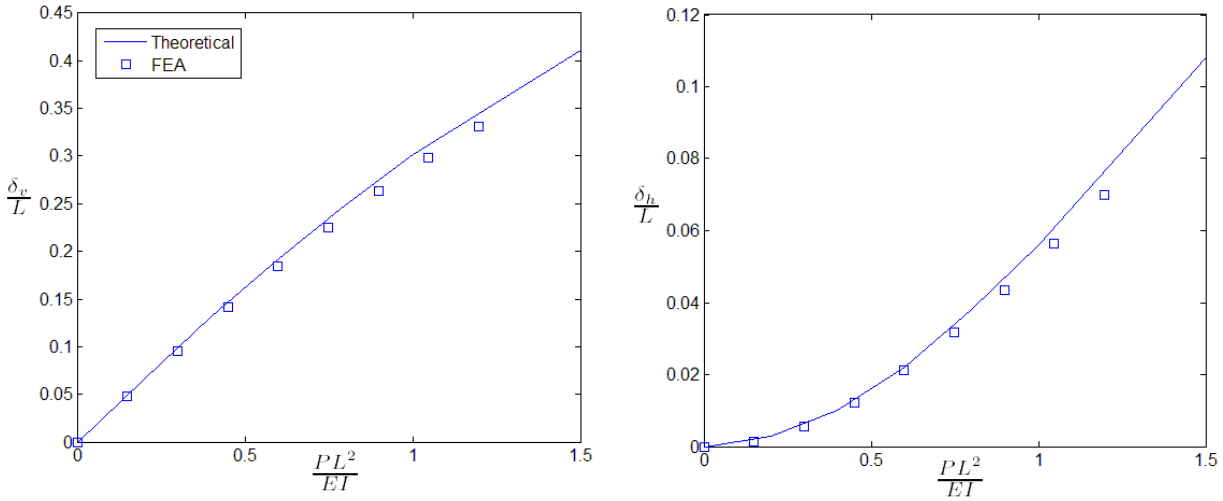

(a) (b)

Figure 4.19: FEA vs. Theoretical Cantilever Beam Large Deflections (a) δ_v/L and (b) δ_h/L

5. Conclusion

5.1 Results

The goal of the research was to collect experimental data on a joined-wing test article's deformation under a follower-force load to validate results obtained from analytical tools such as FEA software or other alternatives like GEBT. In order realize this goal it was necessary to design, build, and test a follower-force load application system capable of varying the direction of the applied load on a test article, and then to come up with a method to ensure a follower-force was applied to the test article of interest. The required test stand, with a FEA analyzed factor of safety of 10, was built and a methodology of applying a follower-force to within 1 deg of the desired direction was created. The data collected from the experiments were compared to a set of analytical results from FEA in order to obtain a quick assessment of differences between follower and stationary direction forces and to validate a set of analytical results on a follower-force analysis.

The first item studied was the qualification test article, which was used to create a set of procedures for applying a follower-force on a test article. The comparison of the data collected to the analytical data showed that follower-force causes larger deformation in the test article when compared to a stationary direction force.

The second item studied was the joined-wing test article, which was designed in a previous study to exhibit a nonlinear bend-twist response prior to permanent deformation. The bend-twist response was captured during the experiment using a laser tracker and strain readings were used to make sure that the test article did not yield. The joined-wing test article was shown to be much stiffer than the qualification test article and was capable of carrying a much higher load even though it was constructed using fore and aft wing of similar dimensions as the qualification test article. The joined-wing test article was loaded to 5.5 times the load seen by the qualification test article, but its maximum measured deformation was 7.36 in as compared to 28.04 in for the qualification test article.

Initial results for the comparison of the follower-force FEA results and experimental data for the qualification and the joined-wing test articles showed that there was a large difference. Some of the possible causes for the differences in the displacements have been discussed in Section 4.3 to include movement in the boundary condition and couple issues with the load application system. However, the most significant cause was determined to be the FEA models used for comparison with the experimental data. The FEA models were tuned to match data collected from a fixed point force experiment, but due to some errors introduced during the tuning process, the 6DOF spring elements used to model the bolt

connections in the test articles were made to be too stiff. As a result, the FEMs of the test articles were made to be much stiffer than the corresponding test articles.

It was shown that adjusting the 6DOF spring elements in the top mounting structures of the test article FEMs resulted in better agreement between the experimental data and the FEA results. After some trial-and-error hand tuning of the spring elements, the follower-force FEA results and experimental data for both test articles were brought to within 1% in terms of total displacement. As a check to verify the validity of the FEMs, the qualification FEM was used to repeat an analysis of a cantilever beam undergoing large deformations. The result of the analysis was checked against theoretical predictions and it was shown that the qualification FEM produced valid results.

Although this study collected data on two simple test articles, the procedures outlined for applying a follower-force and taking deformation measurements could be used on any item of interest.

5.2 Future Work

As noted in Section 4.3, there is an issue with the rotation of the load cell that can cause errors in the load direction. For the joined-wing test article, at 1100 lbs, the possible error was calculated to be as much as 0.3 in for a rotation of 10 degrees from the nominal orientation. Although, this problem can be alleviated by rotating the load cell to the proper orientation by hand, some method of determining the proper orientation other than "eyeballing it" is needed.

Also, discussed in Section 4.3, the FEMs of the both the qualification and joined-wing test articles need to be tuned using the appropriate load data. Although trial-and-error hand tuning was completed on the FEMs to produce a set of data that closely matches the experimental data, further study is need to determine whether the FEMs will continue to provide valid results for different types of loads.

It might be interesting to repeat the non-follower force experiments using the new load application system for the sake of verification. However, considering that the same test articles were used at the same location for the current experiments, it seems highly unlikely that results would be any different. Therefore, although it would be nice to repeat the non-follower force experiments, it probably is not necessary.

The test articles used for this study were of extremely simple designs that are not truly representative of the actual aircraft wing designs. Experiments with more realistic test articles should be conducted in order to facilitate design efforts for actual wings to be used on aircrafts. However, even

without doing any addition experiments on test articles that are more representative of actual wing designs, the data collected in this study should be used to validate any upcoming analytical tools, such as GEBT.

Bibliography

[1] Julian Wolkovich, "The Joined Wing: An Overview," *Journal of Aircraft*, pp. 23(3): 161-178, 1986.

[2] Jonathan D. Boston, "Experiments with Geometric Non-Linear Coupling for Analytical Validation," Air Force Institute of Technology, Master's Thesis Mar 2010.

[3] John W. Gallman and Ilan M. Kroo, "Structural Optimization for Joined-Wing Synthesis," *Journal of Aircraft*, pp. 33(1): 214-233, 1996.

[4] Maxwell Blair, Robert A. Canfield, and Ronald W. Roberts Jr., "Joined-Wing Aeroelastic Design with Geometric Non-Lienarity," *Journal of Aircraft*, pp. 42(4): 832-848, 2005.

[5] Vanessa L. Bond, "Flexible Twist for Pitch Control in a High Altitude Long Endurance Aircraft with Nonlinear Response," Air Force Institute of Technology, PhD Thesis Dec 2008.

[6] Nicholas S. Green, Nick Keller, and Jonathan D. Boston, "Mech 542 Aluminum Joined-Wing Experiment," Air Force Institute of Technology, Final Report for Mech 542 Mar 2009.

[7] Brian Dreibelbis and Jim Barth, "Structural Analysis of Joint Wings," in *AIAA Midaltantic Regional Student Conference*, College Park, Maryland, Apr 2003.

[8] Soujanya Marisarla, "Structural Analysis of an Equivalent Box-Wing Representation of Sensorcraft Joined-Wing Configuration for High-Altitude, Long-Endurance (HALE) Aircraft," University of Cincinnati, Master's Thesis Mar 2005.

[9] Vijay Narayanan, "Structural Analysis of Reinforced Shell Wing Model for Joined-Wing Configuration," University of Cincinnati, Master's Thesis Mar 2005.

[10] Valentina D. Kaloyanova, Karman N. Ghia, and Urmila Ghia, "Structural Modeling and Optimization of the Joined Wing of a High-Altitude Long-Endurance (HALE) Aircraft," in *AIAA Aerospace Sciences Metting and Exhibit*, Reno, Nevada, Jan 2005, pp. AIAA 2005-1087.

[11] Cody C. Rasmussen, Robert A. Canfield, and Maxwell Blair, "Optimization Process for Configuration of Flexible Joined-Wing," in *AIAA/ISSMO Multidisciplinary Analysis and Optimization Conference*, Albany, New York, Aug 2004, pp. AIAA 2004-4330.

[12] Mayuresh J. Patil, "Nonlinear Aeroelastic Analysis of Joined-Wing Aircraft," in *AIAA/ASME/ASCE/AHS Structures, Structural Dynamics, and Materials Conference*, Norfolk, Virginia, Apr 2003, pp. AIAA 2003-1487.

[13] Brandon J. Adams, "Structural Stability of a Joined-Wing SensorCraft," Air Force Institute of Technology, Master's Thesis Jun 2007.

[14] Nicholas S. Green, "Structural Optimization of Joined-Wing Beam Model with Bend-Twist Coupling Using Equivalent Static Loads," Air Force Institute of Technology, Master's Thesis Jun 2009.

[15] James M. Gere and Stephen P. Timoshenko, *Mechanics of Materials*, 3rd ed. Boston, Massachusetts: PWS-Kent, 1990.

REPORT DOCUMENTATION PAGE

Form Approved
OMB No. 0704–0188

1. REPORT DATE (DD–MM–YYYY)	2. REPORT TYPE	3. DATES COVERED *(From — To)*
24 03 2011	Master's Thesis	Jun 2010 – Mar 2011

4. TITLE AND SUBTITLE
Follower-Force Experiments with Geometric Nonlinear Coupling for Analytical Validation

5a. CONTRACT NUMBER
5b. GRANT NUMBER
5c. PROGRAM ELEMENT NUMBER

6. AUTHOR(S)
Kim, Tae H., Capt, USAF

5d. PROJECT NUMBER
5e. TASK NUMBER
5f. WORK UNIT NUMBER

7. PERFORMING ORGANIZATION NAME(S) AND ADDRESS(ES)
Air Force Institute of Technology
Graduate School of Engineering and Management (AFIT/ENY)
2950 Hobson Way
WPAFB OH 45433-7765

8. PERFORMING ORGANIZATION REPORT NUMBER
AFIT/GA/ENY/11-M10

9. SPONSORING / MONITORING AGENCY NAME(S) AND ADDRESS(ES)
Dr. Ned Lindsley (Ned.Lindsley@wpafb.af.mil)
US Air Force Research Laboratory/RBSD
2130 Eighth Street, Building 146
Wright-Patterson AFB 45433-7542
937-255-8452

10. SPONSOR/MONITOR'S ACRONYM(S)
AFRL/RBSD

11. SPONSOR/MONITOR'S REPORT NUMBER(S)

12. DISTRIBUTION / AVAILABILITY STATEMENT
APPROVED FOR PUBLIC RELEASE; DISTRIBUTION UNLIMITED

13. SUPPLEMENTARY NOTES
This material is declared a work of the US government and is not subject to copyright protection in the United States.

14. ABSTRACT

This study was a follow-up of a previous study where static deflection data of a joined-wing test article was collected from a series of experiments using a laser scanner and a laser tracker while the test articles were subjected to follower-forces. One of the goals of this study was to collect accurate experimental data which could be used to validate analytical methods, such as geometrically exact beam theory, which are used to predict the nonlinear response of joined-wings. The load application system used on the previous study was not able to provide a follower-force on the test articles, and therefore the loads were not representative of what the joined-wing would experience under more realistic loading conditions. The test articles used for the experiments are the qualification model and the joined-wing model. The qualification model is simply a thin aluminum beam, which is 72 in long, 8 in wide, and 0.5 in thick, and the joined-wing model is made up of two aluminum beams, which are similar in dimension to the qualification model and are joined at the tip. The qualification model was used mainly for validating the experimental procedures in preparation for the actual experiment on the joined-wing model. The deflection data of the test articles were collected using a laser tracker, and some of the measurement locations were chosen for easy comparison with the results from the previous study. The experimental data is compared to the results obtained using finite element analysis to determine how close the finite element analysis predictions are to the actual data.

15. SUBJECT TERMS
Joined-wing, geometric coupling, experimental methods, bend-twist coupling, GEBT

16. SECURITY CLASSIFICATION OF:			17. LIMITATION OF ABSTRACT	18. NUMBER OF PAGES	19a. NAME OF RESPONSIBLE PERSON
a. REPORT	b. ABSTRACT	c. THIS PAGE	UU	80	Dr. Eric D. Swenson
U	U	U			19b. TELEPHONE NUMBER (Include Area Code) (937)255-3636, ext 7479 Email: eric.swenson@afit.edu